

Multi- π^+ systems in finite volume

Peng Guo^{1,2,*} and Bingwei Long^{3,†}

¹*Department of Physics and Engineering, California State University, Bakersfield, CA 93311, USA*

²*Kawli Institute for Theoretical Physics, University of California, Santa Barbara, CA 93106, USA*

³*College of Physic, Sichuan University, Chengdu, Sichuan 610065, China*

(Dated: February 24, 2020)

We present a formalism to describe two- π^+ and three- π^+ dynamics in finite volume, the formalism is based on combination of a variational approach and the Faddeev method. Both pair-wise and three-body interactions are included in the presentation. Impacts of finite lattice spacing and the cubic lattice symmetry are also discussed. To illustrate application of the formalism, the pair-wise contact interaction that resembles the leading order interaction terms in chiral effective theory is used to analyze recent lattice results.

I. INTRODUCTION

Understanding of few-hadron interactions is crucial in nuclear/hadron physics. Few-hadron dynamics provides a unique access to various fundamental parameters of Quantum Chromodynamics (QCD), for quarks and gluons only manifest themselves within hadrons due to color confinement. For instance, the u - and d -quark mass difference can be extracted from $\eta \rightarrow 3\pi$ decay process [1–7]. Remarkable few-body phenomena, such as the Efimov states [8, 9] and halo nuclei [10, 11], have been predicted and observed in strong-interaction physics. Few-body systems also offer an outlook for many-body effects, e.g., three-nucleon forces [12–14] and fractional quantum Hall effects [15].

Latest advances have now made lattice QCD (LQCD) a powerful quantitative tool to study hadron physics from the first principles. In recent years, realistic LQCD calculations of multi-hadron systems have been made possible [16–27]. However, LQCD calculations are usually performed in a periodic box in the Euclidean space-time, and only discrete energy spectra are extracted from time dependent correlation functions. That is to say, the multi-hadron dynamics is encoded in a set of discrete energy levels in finite volume. Therefore, mapping out infinite-volume few-body dynamics from finite-volume energy spectra is a key step toward understanding multi-hadron systems from LQCD calculations.

In the two-body sector, a pioneering approach proposed by Lüscher [28] tends to build connections between infinite volume reaction amplitudes and energy levels in a periodic cubic box, which was later on further extended to the cases of moving frames and coupled channels [29–38]. In past few years, progresses have been made on the study of few-body systems above three-body thresholds in finite volume [39–67]. To certain extent, most of these developments may be regarded as extensions of the Lüscher formula. Lüscher’s formula in two-body sector may demonstrate a clear advantage: the quantization

condition is given in terms of infinite volume two-body scattering amplitude or phase shift, it provides a direct connection between infinite-volume reaction amplitudes and finite-volume energy spectra. Unfortunately, above three-body threshold, in addition to complication of finite volume dynamics, the infinite volume few-body reaction amplitudes usually can not be easily parameterized in an analytic form, solutions of these amplitudes are given by coupled integral equations, such as Faddeev equations [68, 69]. Dealing with questions regarding infinite and finite-volume physics simultaneously presents great challenges. As illustrated in Ref. [65, 66], the quantization condition of few-body systems may be presented in terms of finite-volume Green’s function and effective interaction between particles embodied by a potential. Since infinite volume scattering amplitudes are not explicitly involved in variational approach, it may be more efficient for practical analysis of LQCD calculation results.

In present work, the variational approach proposed in [64–67] is applied to multi- π^+ systems. In $3\pi^+$ system, both pair-wise interactions and three-body interactions are included in our presentation. We also take into consideration relativistic pion kinematics, the finite lattice spacing and cubic lattice symmetry effects. As our initial attempt, the quantization conditions are used to analyze LQCD data published in Ref. [27] by accounting for only pair-wise contact interaction in the center-of-mass (CM) frame. The $2\pi^+$ scattering length and effective range are extracted from analysis. With a single parameter, the coupling constant of the pair-wise contact interaction, we are able to make prediction on energy spectra, albeit with relatively large uncertainties.

The paper is organized as follows. The formalism of finite volume multi- π^+ systems at the continuum limit, where the lattice spacing vanishes, is presented in detail in Section II. The finite lattice spacing effect and cubic lattice symmetry are discussed in Section III. Numerical results are given in Section IV, followed by a summary in Section V.

* pguo@csu.edu

† bingwei@scu.edu.cn

II. RELATIVISTIC MULTI- π^+ SYSTEMS IN FINITE VOLUME AT CONTINUUM LIMIT

For the future reference, we give in this section a complete presentation of our formalism that describes finite-volume dynamics of multi- π^+ systems. The formalism adopted in this work is based on the variational approach combined with the Faddeev method which was previously discussed in Refs. [64–67]. The relativistic, finite-volume multi- π^+ dynamics is for the moment formulated at the continuum limit with vanishing lattice spacing ($a = 0$), in the sense that ultraviolet divergence is to be removed through proper regularization procedure. The finite lattice spacing effect will be installed rather straight-forwardly later on in Section III. In what follows, we will go through dynamical equations of the two-pion and three-pion systems, and close the section by elaborating how ultraviolet divergences are treated and how renormalization is carried out.

A. Dynamical equations of $2\pi^+$ system

The relativistic $2\pi^+$ system in finite volume is governed by the homogeneous Lippmann-Schwinger (LS) equation [65–67]:

$$\phi_{2\pi}(\mathbf{r}) = \int_{L^3} d\mathbf{r}' G_{2\pi}^{(\mathbf{P})}(\mathbf{r} - \mathbf{r}'; E) V(r') \phi_{2\pi}(\mathbf{r}'), \quad (1)$$

where \mathbf{r} and \mathbf{P} are the relative coordinate and total momentum of the pions, respectively. With the assumption of zero lattice spacing ($a = 0$), \mathbf{r} is continuously distributed in finite volume, and $\int_{L^3} d\mathbf{r}'$ stands for continuous integration bound by the edges of a periodic cubic box. The spherical two-body potential is represented by $V(r)$ where $r = |\mathbf{r}|$. The wave function for relative motion of the two pions satisfies periodic boundary condition [64–66],

$$\phi_{2\pi}(\mathbf{r} + \mathbf{n}L) = e^{-i\frac{\mathbf{P}}{2} \cdot \mathbf{n}L} \phi_{2\pi}(\mathbf{r}), \quad \mathbf{n} \in \mathbb{Z}^3, \quad (2)$$

where L is the size of the cubic lattice. Imposing the the periodic boundary condition on the plane wave of CM motion yields

$$\mathbf{P} = \frac{2\pi}{L} \mathbf{d}, \quad \mathbf{d} \in \mathbb{Z}^3. \quad (3)$$

We remark that throughout the entire paper, the explicit energy dependence of both the wave function and the scattering amplitude is dropped for the convenience of presentation. The two-pion Green's function is given by

$$G_{2\pi}^{(\mathbf{P})}(\mathbf{r}; E) = \sum_{\mathbf{p}} e^{i(\mathbf{p} - \frac{\mathbf{P}}{2}) \cdot \mathbf{r}} \tilde{G}_{2\pi}^{(\mathbf{P})}(\mathbf{p}; E),$$

$$\tilde{G}_{2\pi}^{(\mathbf{P})}(\mathbf{p}; E) = \frac{1}{L^3} \frac{2(E_{\mathbf{p}} + E_{\mathbf{P}-\mathbf{p}})}{2E_{\mathbf{p}}2E_{\mathbf{P}-\mathbf{p}}} \frac{1}{E^2 - (E_{\mathbf{p}} + E_{\mathbf{P}-\mathbf{p}})^2}, \quad (4)$$

where $E_{\mathbf{p}} = \sqrt{m_{\pi}^2 + \mathbf{p}^2}$ and $\mathbf{p} = \frac{2\pi\mathbf{n}}{L}$, $\mathbf{n} \in \mathbb{Z}^3$.

Defining finite-volume two-pion amplitude,

$$t_{2\pi}^{(\mathbf{P})}(\mathbf{k}) = - \int_{L^3} d\mathbf{r} e^{-i(\mathbf{k} - \frac{\mathbf{P}}{2}) \cdot \mathbf{r}} V(r) \phi_{2\pi}(\mathbf{r}), \quad (5)$$

where $\mathbf{k} = \frac{2\pi\mathbf{n}}{L}$, $\mathbf{n} \in \mathbb{Z}^3$, one can transform Eq. (1) into the homogeneous momentum-space LS equation:

$$t_{2\pi}^{(\mathbf{P})}(\mathbf{k}) = \sum_{\mathbf{p}} \tilde{V}(|\mathbf{k} - \mathbf{p}|) \tilde{G}_{2\pi}^{(\mathbf{P})}(\mathbf{p}; E) t_{2\pi}^{(\mathbf{P})}(\mathbf{p}), \quad (6)$$

where the momentum-space potential

$$\tilde{V}(k) = \int_{L^3} d\mathbf{r} e^{-i\mathbf{k} \cdot \mathbf{r}} V(r). \quad (7)$$

According to the variational approach [64–67], the quantization condition for the two-pion system is given by

$$\det \left[\delta_{\mathbf{k}, \mathbf{p}} - \tilde{V}(|\mathbf{k} - \mathbf{p}|) \tilde{G}_{2\pi}^{(\mathbf{P})}(\mathbf{p}; E) \right] = 0,$$

$$(\mathbf{k}, \mathbf{p}) \in \frac{2\pi\mathbf{n}}{L}, \mathbf{n} \in \mathbb{Z}^3. \quad (8)$$

Solving for E yields the discrete energy spectrum of two interacting pions in finite volume at the continuum limit where the lattice space approaches zero.

B. Dynamical equations of $3\pi^+$ system

After factoring out the CM motion (see Appendix D for the example of removing CM motion for a nonrelativistic three-particle system), the dynamics of relativistic finite-volume three-pion system is described by a LS type integral equation in coordinate space,

$$\phi_{3\pi}(\mathbf{r}_{13}, \mathbf{r}_{23}) = \sum_{k=1}^4 \int_{L^3} d\mathbf{r}'_{13} d\mathbf{r}'_{23}$$

$$\times G_{(k)}^{(\mathbf{P})}(\mathbf{r}_{13} - \mathbf{r}'_{13}, \mathbf{r}_{23} - \mathbf{r}'_{23}; E) V_{(k)}(\mathbf{r}'_{13}, \mathbf{r}'_{23}) \phi_{3\pi}(\mathbf{r}'_{13}, \mathbf{r}'_{23}), \quad (9)$$

where $\mathbf{r}_{ij} = \mathbf{x}_i - \mathbf{x}_j$ is relative coordinate between the i -th and j -th pions. \mathbf{r}_{13} and \mathbf{r}_{23} are chosen to describe the relative motion of $3\pi^+$ system. The pair-wise interactions between i -th and j -th identical pions are represented by

$$V_{(k)}(\mathbf{r}_{13}, \mathbf{r}_{23}) = V(r_{ij}), \quad (10)$$

with $k = 1, 2, 3$ and $k \neq i \neq j$ and $V(r)$ is the previously defined two-body potential. $V_{(4)}(\mathbf{r}_{13}, \mathbf{r}_{23})$ with $k = 4$ denotes the three-body force acting on all the pions. The three-pion Green's functions are defined as follows:

$$G_{(k)}^{(\mathbf{P})}(\mathbf{r}_{13}, \mathbf{r}_{23}; E)$$

$$= \sum_{\mathbf{p}_1, \mathbf{p}_2} e^{i(\mathbf{p}_1 - \frac{\mathbf{P}}{2}) \cdot \mathbf{r}_{13}} e^{i(\mathbf{p}_2 - \frac{\mathbf{P}}{2}) \cdot \mathbf{r}_{23}} \tilde{G}_{(k)}^{(\mathbf{P})}(\mathbf{p}_1, \mathbf{p}_2; E), \quad (11)$$

and

$$\begin{aligned}\tilde{G}_{(k)}^{(\mathbf{P})}(\mathbf{p}_1, \mathbf{p}_2; E) &= 2E_{\mathbf{p}_k} \tilde{G}_{3\pi}^{(\mathbf{P})}(\mathbf{p}_1, \mathbf{p}_2; E), \quad k = 1, 2, 3, \\ \tilde{G}_{(4)}^{(\mathbf{P})}(\mathbf{p}_1, \mathbf{p}_2; E) &= \tilde{G}_{3\pi}^{(\mathbf{P})}(\mathbf{p}_1, \mathbf{p}_2; E),\end{aligned}\quad (12)$$

where

$$\tilde{G}_{3\pi}^{(\mathbf{P})}(\mathbf{p}_1, \mathbf{p}_2; E) = \frac{1}{L^6} \frac{2 \sum_{i=1}^3 E_{\mathbf{p}_i}}{2E_{\mathbf{p}_1} 2E_{\mathbf{p}_2} 2E_{\mathbf{p}_3}} \frac{1}{E^2 - (\sum_{i=1}^3 E_{\mathbf{p}_i})^2}.\quad (13)$$

The total momentum

$$\mathbf{P} = \mathbf{p}_1 + \mathbf{p}_2 + \mathbf{p}_3 = \frac{2\pi}{L} \mathbf{d}, \quad \mathbf{d} \in \mathbb{Z}^3, \quad (14)$$

where

$$\mathbf{p}_i = \frac{2\pi \mathbf{n}_i}{L}, \quad \mathbf{n}_i \in \mathbb{Z}^3, \quad (15)$$

is the momentum of the i -th particle. The relativistic kinematic factors, $2E_{\mathbf{p}_k}$ for $k = 1, 2, 3$, in Eq.(12) are associated with the relativistic normalization of the free propagating spectator particle in presence of the pair-wise interaction between the i -th and j -th particles. The relativistic LS equation may be derived from the Bethe-Salpeter equation, see Appendix A. The three-body wave function must satisfy the periodic boundary condition [66]:

$$\phi_{3\pi}(\mathbf{r}_{13} + \mathbf{n}_1 L, \mathbf{r}_{23} + \mathbf{n}_2 L) = e^{-i\frac{\mathbf{P}}{3} \cdot (\mathbf{n}_1 L + \mathbf{n}_2 L)} \phi_{3\pi}(\mathbf{r}_{13}, \mathbf{r}_{23}), \quad (16)$$

where $\mathbf{n}_{1,2} \in \mathbb{Z}^3$.

As suggested in Refs. [64–67], the Faddeev amplitudes may be introduced by

$$\begin{aligned}t_{(k)}^{(\mathbf{P})}(\mathbf{k}_1, \mathbf{k}_2) &= - \int_{L^3} d\mathbf{r}_{13} d\mathbf{r}_{23} e^{-i(\mathbf{k}_1 - \frac{\mathbf{P}}{3}) \cdot \mathbf{r}_{13}} e^{-i(\mathbf{k}_2 - \frac{\mathbf{P}}{3}) \cdot \mathbf{r}_{23}} \\ &\quad \times V(r_{ij}) \phi_{3\pi}(\mathbf{r}_{13}, \mathbf{r}_{23}), \quad k \neq i \neq j, \\ t_{(4)}^{(\mathbf{P})}(\mathbf{k}_1, \mathbf{k}_2) &= - \int_{L^3} d\mathbf{r}_{13} d\mathbf{r}_{23} e^{-i(\mathbf{k}_1 - \frac{\mathbf{P}}{3}) \cdot \mathbf{r}_{13}} e^{-i(\mathbf{k}_2 - \frac{\mathbf{P}}{3}) \cdot \mathbf{r}_{23}} \\ &\quad \times V_{(4)}(\mathbf{r}_{13}, \mathbf{r}_{23}) \phi_{3\pi}(\mathbf{r}_{13}, \mathbf{r}_{23}).\end{aligned}\quad (17)$$

Equation (9) is thus turned into coupled equations:

$$\begin{aligned}t_{(k)}^{(\mathbf{P})}(\mathbf{k}_1, \mathbf{k}_2) &= \sum_{\mathbf{p}_1, \mathbf{p}_2} \tilde{V}_{(k)}(\mathbf{k}_1 - \mathbf{p}_1, \mathbf{k}_2 - \mathbf{p}_2) \\ &\quad \times \tilde{G}_{3\pi}^{(\mathbf{P})}(\mathbf{p}_1, \mathbf{p}_2; E) \left[\sum_{k'=1}^3 2E_{\mathbf{p}_{k'}} t_{(k')}^{(\mathbf{P})}(\mathbf{p}_1, \mathbf{p}_2) + t_{(4)}^{(\mathbf{P})}(\mathbf{p}_1, \mathbf{p}_2) \right],\end{aligned}\quad (18)$$

where $\tilde{V}_{(k)}$'s are the Fourier transform of pair-wise and three-body interaction potentials,

$$\begin{aligned}\tilde{V}_{(k)}(\mathbf{k}_1, \mathbf{k}_2) &= \int_{L^3} d\mathbf{r}_{13} d\mathbf{r}_{23} e^{-i\mathbf{k}_1 \cdot \mathbf{r}_{13}} e^{-i\mathbf{k}_2 \cdot \mathbf{r}_{23}} V(r_{ij}) \Big|_{k=1,2,3}^{k \neq i \neq j}, \\ \tilde{V}_{(4)}(\mathbf{k}_1, \mathbf{k}_2) &= \int_{L^3} d\mathbf{r}_{13} d\mathbf{r}_{23} e^{-i\mathbf{k}_1 \cdot \mathbf{r}_{13}} e^{-i\mathbf{k}_2 \cdot \mathbf{r}_{23}} V_{(4)}(\mathbf{r}_{13}, \mathbf{r}_{23}).\end{aligned}\quad (19)$$

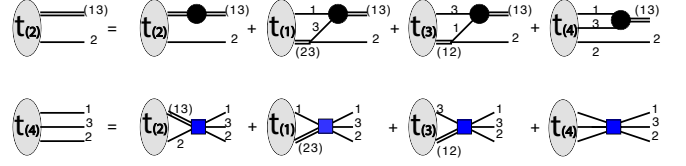


FIG. 1: Diagrammatic representation of Eq.(25) and Eq.(26), pair-wise and three-body interactions are represented by black solid circle and blue solid square.

Two-body interactions $\tilde{V}_{(1,2,3)}$ are related to $\tilde{V}(k)$, as defined in Eq. (7), through

$$\begin{aligned}\tilde{V}_{(2)}(\mathbf{k}_1, \mathbf{k}_2) &= \tilde{V}(k_1) L^3 \delta_{\mathbf{k}_2, \mathbf{0}}, \\ \tilde{V}_{(1)}(\mathbf{k}_1, \mathbf{k}_2) &= \tilde{V}(k_2) L^3 \delta_{\mathbf{k}_1, \mathbf{0}}, \\ \tilde{V}_{(3)}(\mathbf{k}_1, \mathbf{k}_2) &= \tilde{V}\left(\frac{|\mathbf{k}_1 - \mathbf{k}_2|}{2}\right) L^3 \delta_{\mathbf{k}_1, -\mathbf{k}_2},\end{aligned}\quad (20)$$

where $\delta_{\mathbf{k}, \mathbf{p}}$ denotes the 3D Kronecker delta function.

1. Exchange symmetry of $3\pi^+$ system

As is the case for any identical bosons, the wave function of $3\pi^+$ system must be invariant under exchange of any pair of pions, for example,

$$\phi_{3\pi}(\mathbf{r}_{13}, \mathbf{r}_{23}) \stackrel{1 \leftrightarrow 3}{=} \phi_{3\pi}(\mathbf{r}_{31}, \mathbf{r}_{21}) \stackrel{2 \leftrightarrow 1}{=} \phi_{3\pi}(\mathbf{r}_{12}, \mathbf{r}_{32}), \quad (21)$$

and $\phi_{3\pi}(\mathbf{r}_{ik}, \mathbf{r}_{jk}) \stackrel{i \leftrightarrow j}{=} \phi_{3\pi}(\mathbf{r}_{jk}, \mathbf{r}_{ik})$. The exchange symmetry of three-body wave function suggests that $t_{(1,2,3)}^{(\mathbf{P})}$ are related:

$$\begin{aligned}t_{(1)}^{(\mathbf{P})}(\mathbf{k}_1, \mathbf{k}_2) &= t_{(2)}^{(\mathbf{P})}(\mathbf{k}_2, \mathbf{k}_1), \\ t_{(3)}^{(\mathbf{P})}(\mathbf{k}_1, \mathbf{k}_2) &= t_{(2)}^{(\mathbf{P})}(\mathbf{k}_1, \mathbf{k}_3) = t_{(2)}^{(\mathbf{P})}(\mathbf{k}_2, \mathbf{k}_3),\end{aligned}\quad (22)$$

where $\mathbf{P} = \mathbf{k}_1 + \mathbf{k}_2 + \mathbf{k}_3$.

Using the definition of $t_{(2)}^{(\mathbf{P})}$ in Eq.(17) and symmetry relations of wave function in Eq.(21), we find useful symmetry properties of $t_{(2)}^{(\mathbf{P})}$:

$$t_{(2)}^{(\mathbf{P})}(\mathbf{k}_3, \mathbf{k}_2) = t_{(2)}^{(\mathbf{P})}(\mathbf{k}_1, \mathbf{k}_2), \quad t_{(2)}^{(\mathbf{P})}(\mathbf{k}_3, \mathbf{k}_1) = t_{(2)}^{(\mathbf{P})}(\mathbf{k}_2, \mathbf{k}_1). \quad (23)$$

In addition to that of the wave function, exchange symmetry of three-body potential $V_{(4)}$ also constrains the amplitude $t_{(4)}$:

$$t_{(4)}^{(\mathbf{P})}(\mathbf{k}_1, \mathbf{k}_2) = t_{(4)}^{(\mathbf{P})}(\mathbf{k}_2, \mathbf{k}_1) = t_{(4)}^{(\mathbf{P})}(\mathbf{k}_1, \mathbf{k}_3) = \dots \quad (24)$$

2. Further reduction of $3\pi^+$ LS equations

Using the aforementioned symmetry relations of Faddeev amplitudes, Eq.(18) are further reduced into the

following equations:

$$t_{(2)}^{(\mathbf{P})}(\mathbf{k}_1, \mathbf{k}_2) = \sum_{\mathbf{p}_1} \tilde{V}(|\mathbf{k}_1 - \mathbf{p}_1|) L^3 \tilde{G}_{3\pi}^{(\mathbf{P})}(\mathbf{p}_1, \mathbf{k}_2; E) \\ \times \left[2E_{\mathbf{k}_2} t_{(2)}^{(\mathbf{P})}(\mathbf{p}_1, \mathbf{k}_2) + 2E_{\mathbf{p}_1} t_{(2)}^{(\mathbf{P})}(\mathbf{k}_2, \mathbf{p}_1) \right. \\ \left. + 2E_{\mathbf{P}-\mathbf{p}_1-\mathbf{k}_2} t_{(2)}^{(\mathbf{P})}(\mathbf{p}_1, \mathbf{P} - \mathbf{p}_1 - \mathbf{k}_2) + t_{(4)}^{(\mathbf{P})}(\mathbf{p}_1, \mathbf{k}_2) \right], \quad (25)$$

and

$$t_{(4)}^{(\mathbf{P})}(\mathbf{k}_1, \mathbf{k}_2) = \sum_{\mathbf{p}_1, \mathbf{p}_2} \tilde{V}_{(4)}(\mathbf{k}_1 - \mathbf{p}_1, \mathbf{k}_2 - \mathbf{p}_2) \tilde{G}_{3\pi}^{(\mathbf{P})}(\mathbf{p}_1, \mathbf{p}_2; E) \\ \times \left[2E_{\mathbf{p}_2} t_{(2)}^{(\mathbf{P})}(\mathbf{p}_1, \mathbf{p}_2) + 2E_{\mathbf{p}_1} t_{(2)}^{(\mathbf{P})}(\mathbf{p}_2, \mathbf{p}_1) \right. \\ \left. + 2E_{\mathbf{P}-\mathbf{p}_1-\mathbf{p}_2} t_{(2)}^{(\mathbf{P})}(\mathbf{p}_1, \mathbf{P} - \mathbf{p}_1 - \mathbf{p}_2) + t_{(4)}^{(\mathbf{P})}(\mathbf{p}_1, \mathbf{p}_2) \right]. \quad (26)$$

The diagrammatic representations of Eq.(25) and Eq.(26) are shown in Fig. 1. It may be convenient to consolidate Eqs.(25) and (26) in the matrix form:

$$\begin{bmatrix} t_{(2)}^{(\mathbf{P})}(\mathbf{k}_1, \mathbf{k}_2) \\ t_{(4)}^{(\mathbf{P})}(\mathbf{k}_1, \mathbf{k}_2) \end{bmatrix} = \sum_{\mathbf{p}_1, \mathbf{p}_2} \tilde{G}_{3\pi}^{(\mathbf{P})}(\mathbf{p}_1, \mathbf{p}_2; E) \\ \times \mathcal{K}(\mathbf{k}_1, \mathbf{k}_2; \mathbf{p}_1, \mathbf{p}_2) \begin{bmatrix} t_{(2)}^{(\mathbf{P})}(\mathbf{p}_1, \mathbf{p}_2) \\ t_{(4)}^{(\mathbf{P})}(\mathbf{p}_1, \mathbf{p}_2) \end{bmatrix}, \quad (27)$$

where $(\mathbf{k}_i, \mathbf{p}_i) \in \frac{2\pi\mathbf{n}}{L}, \mathbf{n} \in \mathbb{Z}^3$. Elements of the matrix function $\mathcal{K}(\mathbf{k}_1, \mathbf{k}_2; \mathbf{p}_1, \mathbf{p}_2)$ are given by

$$\mathcal{K}_{11}(\mathbf{k}_1, \mathbf{k}_2; \mathbf{p}_1, \mathbf{p}_2) = 2E_{\mathbf{p}_2} L^3 \left[\delta_{\mathbf{p}_2, \mathbf{k}_2} \tilde{V}(|\mathbf{k}_1 - \mathbf{p}_1|) \right. \\ \left. + \delta_{\mathbf{p}_1, \mathbf{k}_2} \left(\tilde{V}(|\mathbf{k}_1 - \mathbf{p}_2|) + \tilde{V}(|\mathbf{k}_1 - \mathbf{p}_3|) \right) \right], \\ \mathcal{K}_{12}(\mathbf{k}_1, \mathbf{k}_2; \mathbf{p}_1, \mathbf{p}_2) = L^3 \delta_{\mathbf{p}_2, \mathbf{k}_2} \tilde{V}(|\mathbf{k}_1 - \mathbf{p}_1|), \\ \mathcal{K}_{21}(\mathbf{k}_1, \mathbf{k}_2; \mathbf{p}_1, \mathbf{p}_2) = 2E_{\mathbf{p}_2} \left[\tilde{V}_{(4)}(\mathbf{k}_1 - \mathbf{p}_1, \mathbf{k}_2 - \mathbf{p}_2) \right. \\ \left. + \tilde{V}_{(4)}(\mathbf{k}_1 - \mathbf{p}_2, \mathbf{k}_2 - \mathbf{p}_1) + \tilde{V}_{(4)}(\mathbf{k}_1 - \mathbf{p}_3, \mathbf{k}_2 - \mathbf{p}_1) \right], \\ \mathcal{K}_{22}(\mathbf{k}_1, \mathbf{k}_2; \mathbf{p}_1, \mathbf{p}_2) = \tilde{V}_{(4)}(\mathbf{k}_1 - \mathbf{p}_1, \mathbf{k}_2 - \mathbf{p}_2). \quad (28)$$

The coupled equations, Eqs.(25) and (26), or the matrix form of them Eq.(27), will serve as basic dynamical equations for $3\pi^+$ system. The entire $3\pi^+$ energy spectrum in a cubic box can be produced by the quantization condition from Eq.(27):

$$\det \left[\mathbb{I} - \tilde{G}^{(\mathbf{P})} \mathcal{K} \right] = 0. \quad (29)$$

More technical aspects need to be spelled out in order to apply the above quantization condition: renormalization procedure, projection of the spectrum according to

irreducible representations of cubic symmetry group, and finite lattice spacing effect. All these mentioned factors hence ultimately will add extra layer of technical complication on top of Eq.(27). As a simply illustration of our formalism, a specific choice about interactions is made in this work: the two-body potential is the zero-range potential and the three-body interaction is turned off. The contact interaction resembles the leading order terms of the chiral Lagrangian [47, 48, 70]. With contact interaction, the $3\pi^+$ LS equation is simplified considerably. We now turn to renormalization of the multi- π^+ LS equations.

C. Pair-wise contact interaction and renormalization

Since contact interactions allow particles to get arbitrarily close to each other, it is often necessary to regularize the ultraviolet part of the dynamics. This is indeed the case with our illustrative choice of multiple-pion interactions. We will discuss renormalization of both $2\pi^+$ and $3\pi^+$ LS equations in what follows.

1. Renormalization of $2\pi^+$ LS equation

The zero-range potential, $V(r) = V_0 \delta(\mathbf{r})$ and $\tilde{V}(k) = V_0$, is the simplest case of separable potentials. More specifically in this case,

$$t_{2\pi}^{(\mathbf{P})}(\mathbf{k}) \equiv t_{2\pi}^{(\mathbf{P})} \quad (30)$$

is independent of \mathbf{k} for fixed E , and is factored out of the two-body homogeneous LS equation (6):

$$1 = V_0 \sum_{\mathbf{p}} \tilde{G}_{2\pi}^{(\mathbf{P})}(\mathbf{p}; E). \quad (31)$$

The infinite momentum sum of two-pion Green's function (4) is divergent, and the divergence can be regularized by imposing a sharp ultraviolet momentum cutoff Λ . It is instructive to display the divergence in infinite volume and at the continuum limit:

$$\sum_{|\mathbf{p}| < \Lambda} \tilde{G}_{2\pi}^{(0)}(\mathbf{p}; 0) \xrightarrow{L \rightarrow \infty} -\frac{1}{8\pi^2} \int^\Lambda dp \frac{p^2}{E_{\mathbf{p}}^3} \\ \xrightarrow{\Lambda \rightarrow \infty} -\frac{1}{8\pi^2} \ln \frac{\Lambda}{m_\pi} + \frac{1 - \ln 2}{8\pi^2}. \quad (32)$$

For finite values of \mathbf{P} and E , the divergence remains same, or equivalently, adds corrections in powers of P/Λ and $\sqrt{m_\pi E}/\Lambda$. The cutoff dependence of

$$\sum_{|\mathbf{p}| < \Lambda} \tilde{G}_{2\pi}^{(\mathbf{P})}(\mathbf{p}; E = 0)$$

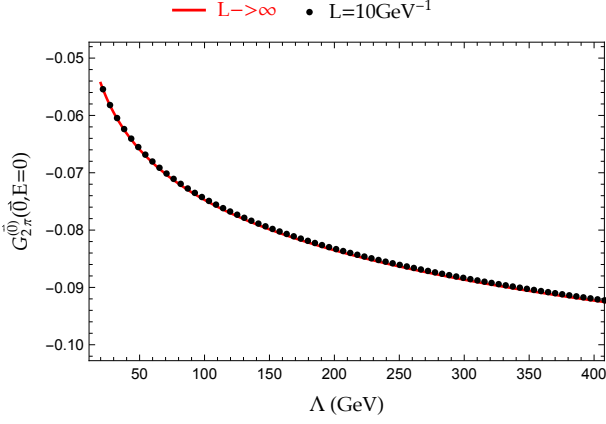


FIG. 2: Plot of cutoff dependence of $\sum_{\mathbf{p}}^{|\mathbf{p}|<\Lambda} \tilde{G}_{2\pi}^{(0)}(\mathbf{p}; 0)$ (black dots) vs. $\frac{1}{8\pi^2}(1 - \ln \frac{2\Lambda}{m_\pi})$ (red curve), where $L = 10\text{GeV}^{-1}$ and $m_\pi = 0.200\text{GeV}$. The black dots are shifted by a constant value: $\sum_{\mathbf{p}}^{|\mathbf{p}|<\Lambda_0} \tilde{G}_{2\pi}^{(0)}(\mathbf{p}; 0) - \frac{1}{8\pi^2}(1 - \ln \frac{2\Lambda_0}{m_\pi})$, where $\Lambda_0 = \frac{40\pi\sqrt{3}}{L}$, so that black dots and red curve overlap when $\Lambda = \Lambda_0$.

compared with its infinite-volume counterpart,

$$-\frac{1}{8\pi^2} \int^\Lambda dp \frac{p^2}{E_p^3} \xrightarrow{\Lambda \rightarrow \infty} \frac{1}{8\pi^2} (1 - \ln \frac{2\Lambda}{m_\pi}),$$

as $\Lambda \rightarrow \infty$, is shown in Fig. 2.

Finite lattice spacing provides a natural regularization on ultraviolet divergence. The physical observables must not depend on the cutoff or choice of lattice spacing, and this is to be assured by renormalization procedure. The bare interaction strength, V_0 , must be redefined to absorb ultraviolet divergence of the momentum sum of Green's function by

$$\frac{1}{V_0} = \frac{1}{V_R(\mu)} + \sum_{\mathbf{p}}^{|\mathbf{p}|<\Lambda} \tilde{G}_{2\pi}^{(0)}(\mathbf{p}; \mu), \quad (33)$$

where $V_R(\mu)$ stands for the renormalized physical coupling strength at the renormalization scale, μ . The two-body quantization condition (31) can be rewritten with the renormalized coupling as

$$\frac{1}{V_R(\mu)} = \sum_{\mathbf{p}}^{|\mathbf{p}|<\Lambda} \tilde{G}_{2\pi}^{(\mathbf{P})}(\mathbf{p}; E) - \sum_{\mathbf{p}}^{|\mathbf{p}|<\Lambda} \tilde{G}_{2\pi}^{(0)}(\mathbf{p}; \mu), \quad (34)$$

where the cutoff dependencies from the summations on the right-hand side cancel out at the limit $\Lambda \rightarrow \infty$, so ultraviolet divergence is now removed from the quantization condition.

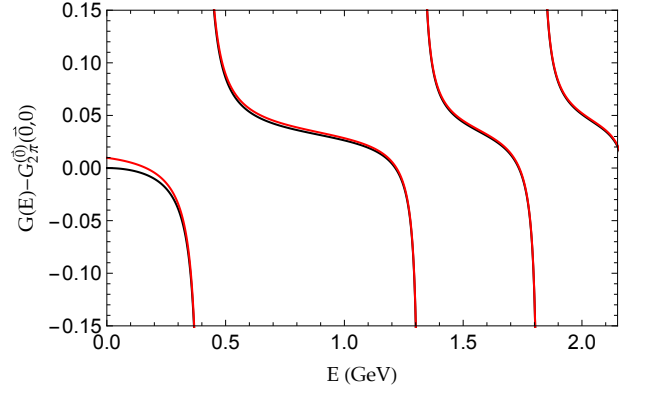


FIG. 3: Plot of $\sum_{\mathbf{p}}^{|\mathbf{p}|<\Lambda} [\tilde{G}_{2\pi}^{(0)}(\mathbf{p}; E) - \tilde{G}_{2\pi}^{(0)}(\mathbf{p}; \mu)]$ (black curve) vs. $\sum_{\mathbf{p}}^{|\mathbf{p}|<\Lambda} [2E_0 L^3 \tilde{G}_{3\pi}^{(0)}(\mathbf{p}, \mathbf{0}; E + 2m_\pi) - \tilde{G}_{2\pi}^{(0)}(\mathbf{p}; \mu)]$ (red curve) with $\mu = 0\text{GeV}$, $L = 10\text{GeV}^{-1}$ and $m_\pi = 0.200\text{GeV}$.

2. Renormalization of $3\pi^+$ LS equation

With three-body interaction $V_{(4)}$ turned off, $t_{(4)}^{(\mathbf{P})}$ vanishes in Eqs. (25) and (26). Due to the zero-range nature of the interaction, the amplitude $t_{(2)}^{(\mathbf{P})}(\mathbf{k}_1, \mathbf{k}_2)$ associated with two-pion interaction between the pair (13) depends only on momentum \mathbf{k}_2 . So it is appropriate to rename $t_{(2)}^{(\mathbf{P})}(\mathbf{k}_1, \mathbf{k}_2)$ as

$$t_{3\pi}^{(\mathbf{P})}(\mathbf{k}_2) = t_{(2)}^{(\mathbf{P})}(\mathbf{k}_1, \mathbf{k}_2). \quad (35)$$

The $3\pi^+$ LS equation (27) is therefore reduced to

$$\begin{aligned} & \left[1 - V_0 \sum_{\mathbf{p}} 2E_{\mathbf{k}_2} L^3 \tilde{G}_{3\pi}^{(\mathbf{P})}(\mathbf{p}, \mathbf{k}_2; E) \right] t_{3\pi}^{(\mathbf{P})}(\mathbf{k}_2) \\ & = 2V_0 \sum_{\mathbf{p}} 2E_{\mathbf{p}} L^3 \tilde{G}_{3\pi}^{(\mathbf{P})}(\mathbf{p}, \mathbf{k}_2; E) t_{3\pi}^{(\mathbf{P})}(\mathbf{p}). \end{aligned} \quad (36)$$

The first line of Eq.(36) describes interaction within the pair (13), with the second pion acting as the spectator. The second line of Eq.(36) represents crossed-channel interactions through exchanging the second particle between the pairs. The direct-channel terms in Eq.(36) resemble the leading order isobar contribution in Khuri-Treiman approach [71–77]. The crossed-channel terms are associated with rescattering corrections from other pairs into isobar pair (13). It can be illustrated quite straightforwardly by iterations of Eq.(36) that crossed-channel contributions are not UV divergent, and that the UV divergence emerge only in direct-channel term. So, as far as renormalization is concerned, crossed-channel interactions can be “turned off”. We arrive at an equation

similar to Eq. (31):

$$1 = V_0 \sum_{\mathbf{p}} 2E_{\mathbf{k}_2} L^3 \tilde{G}_{3\pi}^{(\mathbf{P})}(\mathbf{p}, \mathbf{k}_2; E), \quad (37)$$

where \mathbf{k}_2 is momentum of the spectator pion. Equations (37) and (31) are not identical due to the relativistic kinematics brought by the spectator particle on top of the pair (13):

$$\begin{aligned} & 2E_{\mathbf{k}_2} L^3 \tilde{G}_{3\pi}^{(\mathbf{P})}(\mathbf{k}_1, \mathbf{k}_2; E) \\ &= \frac{1}{L^3} \frac{2(E_{\mathbf{k}_1} + E_{\mathbf{k}_3} + E_{\mathbf{k}_2})}{2E_{\mathbf{k}_1} 2E_{\mathbf{k}_3}} \frac{1}{E^2 - (E_{\mathbf{k}_1} + E_{\mathbf{k}_3} + E_{\mathbf{k}_2})^2}, \end{aligned} \quad (38)$$

compared to

$$\tilde{G}_{2\pi}^{(\mathbf{P})}(\mathbf{k}_1; E) = \frac{1}{L^3} \frac{2(E_{\mathbf{k}_1} + E_{\mathbf{k}_3})}{2E_{\mathbf{k}_1} 2E_{\mathbf{k}_3}} \frac{1}{E^2 - (E_{\mathbf{k}_1} + E_{\mathbf{k}_3})^2}, \quad (39)$$

where $\mathbf{P} = \mathbf{k}_1 + \mathbf{k}_3$ is the total momentum of the pair (13). Nonetheless, the multi-particle Green's function is dominated by the location of poles of particles propagator, so the dominant contributions of the $2\pi^+$ and $3\pi^+$ Green's functions behave in a similar way,

$$\begin{aligned} & 2E_{\mathbf{k}_2} L^3 \tilde{G}_{3\pi}^{(\mathbf{P})}(\mathbf{k}_1, \mathbf{k}_2; E) \\ & \sim \frac{1}{L^3} \frac{1}{2E_{\mathbf{k}_1} 2E_{\mathbf{k}_3}} \frac{1}{E - (E_{\mathbf{k}_1} + E_{\mathbf{k}_3} + E_{\mathbf{k}_2})}, \end{aligned} \quad (40)$$

and

$$\tilde{G}_{2\pi}^{(\mathbf{P})}(\mathbf{k}_1; E) \sim \frac{1}{L^3} \frac{1}{2E_{\mathbf{k}_1} 2E_{\mathbf{k}_3}} \frac{1}{E - (E_{\mathbf{k}_1} + E_{\mathbf{k}_3})}. \quad (41)$$

Therefore, the asymptotic high energy behavior of infinite momentum sum in Eq.(37) and Eq.(31) should be exactly same, with a momentum cutoff,

$$\sum_{\mathbf{p}}^{|\mathbf{p}| < \Lambda} 2E_{\mathbf{k}_2} L^3 \tilde{G}_{3\pi}^{(\mathbf{P})}(\mathbf{p}, \mathbf{k}_2; 0) \sim -\frac{1}{8\pi^2} \ln \frac{\Lambda}{m_\pi} + \text{finite part}. \quad (42)$$

The renormalization procedure in $3\pi^+$ LS equation thus can be carried out in the same way as in the $2\pi^+$ sector, see Fig. 3 for the comparison of

$$\sum_{\mathbf{p}}^{|\mathbf{p}| < \Lambda} \left[\tilde{G}_{2\pi}^{(0)}(\mathbf{p}; E) - \tilde{G}_{2\pi}^{(0)}(\mathbf{p}; \mu) \right]$$

and

$$\sum_{\mathbf{p}}^{|\mathbf{p}| < \Lambda} \left[2E_0 L^3 \tilde{G}_{3\pi}^{(0)}(\mathbf{p}, \mathbf{0}; E + 2m_\pi) - \tilde{G}_{2\pi}^{(0)}(\mathbf{p}; \mu) \right].$$

Using Eq.(33) and redefining the bare coupling V_0 , the renormalized $3\pi^+$ LS equation can be given in a compact form:

$$t_{3\pi}^{(\mathbf{P})}(\mathbf{k}) = 2 \sum_{\mathbf{p}}^{|\mathbf{p}| < \Lambda} \frac{2E_{\mathbf{p}} L^3 \tilde{G}_{3\pi}^{(\mathbf{P})}(\mathbf{p}, \mathbf{k}; E)}{\frac{1}{V_R(\mu)} - \tilde{S}_{3\pi}^{(\mathbf{P})}(\mathbf{k}; E, \mu)} t_{3\pi}^{(\mathbf{P})}(\mathbf{p}), \quad (43)$$

where

$$\tilde{S}_{3\pi}^{(\mathbf{P})}(\mathbf{k}; E, \mu) = \sum_{\mathbf{p}}^{|\mathbf{p}| < \Lambda} \left[2E_{\mathbf{k}} L^3 \tilde{G}_{3\pi}^{(\mathbf{P})}(\mathbf{p}, \mathbf{k}; E) - \tilde{G}_{2\pi}^{(0)}(\mathbf{p}; \mu) \right]. \quad (44)$$

The quantization condition of $3\pi^+$ can be rewritten with the renormalized coupling as

$$\det \left[\delta_{\mathbf{k}, \mathbf{p}} - 2 \frac{2E_{\mathbf{p}} L^3 \tilde{G}_{3\pi}^{(\mathbf{P})}(\mathbf{p}, \mathbf{k}; E)}{\frac{1}{V_R(\mu)} - \tilde{S}_{3\pi}^{(\mathbf{P})}(\mathbf{k}; E, \mu)} \right] = 0, \quad (\mathbf{k}, \mathbf{p}) \in \frac{2\pi \mathbf{n}}{L}, \mathbf{n} \in \mathbb{Z}^3, \quad (45)$$

which yields entire discrete energy spectrum of three pions in a finite box at continuum limit.

III. MULTI- π^+ DYNAMICS WITH FINITE LATTICE SPACING

The lattice QCD simulations are usually performed in a cubic box with finite lattice spacing. We discuss in this section impacts of finite lattice spacing and cubic lattice symmetry on multi- π^+ energy spectra.

A. Finite lattice spacing effect

With a finite lattice spacing a , the coordinate of particles become discrete, a continuous integration over coordinates must be replaced by a discrete sum over lattice sites:

$$\int_{L^3} d\mathbf{r} \rightarrow a^3 \sum_{\mathbf{n}}, \quad (46)$$

where the sum of \mathbf{n} is finite and is bound by the lattice spacing a :

$$(n_x, n_y, n_z) \in [-N, N] \text{ and } N = \frac{L}{2a} - 1.$$

The infinite momentum sum $\sum_{\mathbf{p}}$ where $\mathbf{p} = \frac{2\pi}{L} \mathbf{n}$ and $\mathbf{n} \in \mathbb{Z}^3$ at continuum limit is replaced by a finite sum with momenta restricted to the first Brillouin zone: $(n_x, n_y, n_z) \in [-N, N]$.

In addition, the continuous relativistic energy momentum dispersion relation, $E_{\mathbf{p}} = \sqrt{m_\pi^2 + \mathbf{p}^2}$, is replaced by lattice dispersion relation with a explicit dependence on the finite lattice spacing a ,

$$2 \sinh \frac{aE_{\mathbf{p}}}{2} = \sqrt{2 \cosh am_\pi + 4 - 2 \sum_{i=x,y,z} \cos ap_i}, \quad (47)$$

where $p_i = \frac{2\pi}{L} n_i$, $i = x, y, z$ and $n_i \in [-N, N]$. Therefore, to convert all the continuum limit multi- π^+ dynamical equations presented in Section II to equations with

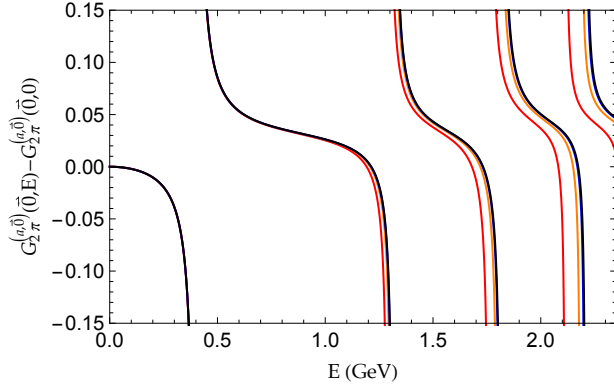


FIG. 4: Plot of $\sum_{\mathbf{p}} \left[\tilde{G}_{2\pi}^{(a,0)}(\mathbf{p}; E) - \tilde{G}_{2\pi}^{(a,0)}(\mathbf{p}; \mu) \right]$ for various finite lattice spacing a 's with $\mu = 0\text{GeV}$, $L = 10\text{GeV}^{-1}$ and $m_\pi = 0.200\text{GeV}$: $a = 0.48\text{GeV}^{-1}$ (Red), 0.24GeV^{-1} (Orange), 0.12GeV^{-1} (Blue), and 0GeV^{-1} (Black).

explicit finite lattice spacing effect build in, the following relations between the physical quantities at continuum limit and their finite lattice spacing counterparts must be considered:

$$E \leftrightarrow \frac{2}{a} \sinh \frac{aE}{2}, \quad m_\pi \leftrightarrow \frac{2}{a} \sinh \frac{am_\pi}{2}, \quad p_i \leftrightarrow \frac{2}{a} \sin \frac{ap_i}{2}. \quad (48)$$

For examples, the momentum space Green's function defined in Eq.(4) and Eq.(13) are now replaced by finite lattice spacing correspondences,

$$\begin{aligned} \tilde{G}_{2\pi}^{(a,\mathbf{P})}(\mathbf{p}; E) &= \frac{a^3}{L^3} \frac{2(2 \sinh \frac{aE_{\mathbf{p}}}{2} + 2 \sinh \frac{aE_{\mathbf{p}-\mathbf{p}}}{2})}{4 \sinh \frac{aE_{\mathbf{p}}}{2} 4 \sinh \frac{aE_{\mathbf{p}-\mathbf{p}}}{2}} \\ &\times \frac{1}{(2 \sinh \frac{aE}{2})^2 - (2 \sinh \frac{aE_{\mathbf{p}}}{2} + 2 \sinh \frac{aE_{\mathbf{p}-\mathbf{p}}}{2})^2}, \quad (49) \end{aligned}$$

for $2\pi^+$, and

$$\begin{aligned} \tilde{G}_{3\pi}^{(a,\mathbf{P})}(\mathbf{p}_1, \mathbf{p}_2; E) &= \frac{a^4}{L^6} \frac{2(\sum_{i=1}^3 2 \sinh \frac{aE_{\mathbf{p}_i}}{2})}{4 \sinh \frac{aE_{\mathbf{p}_1}}{2} 4 \sinh \frac{aE_{\mathbf{p}_2}}{2} 4 \sinh \frac{aE_{\mathbf{p}_3}}{2}} \\ &\times \frac{1}{(2 \sinh \frac{aE}{2})^2 - (\sum_{i=1}^3 2 \sinh \frac{aE_{\mathbf{p}_i}}{2})^2}, \quad (50) \end{aligned}$$

for $3\pi^+$, where $\mathbf{p}_3 = \mathbf{P} - \mathbf{p}_1 - \mathbf{p}_2$. The symbol a in superscript is used to label the functions defined with a finite lattice spacing. The examples of finite lattice spacing effects are illustrated in Fig. 4 and Fig. 5.

1. $2\pi^+$ LS equation with finite lattice spacing

With all the ingredients mentioned previously, the $2\pi^+$ LS equation for a general potential at a finite lattice spac-

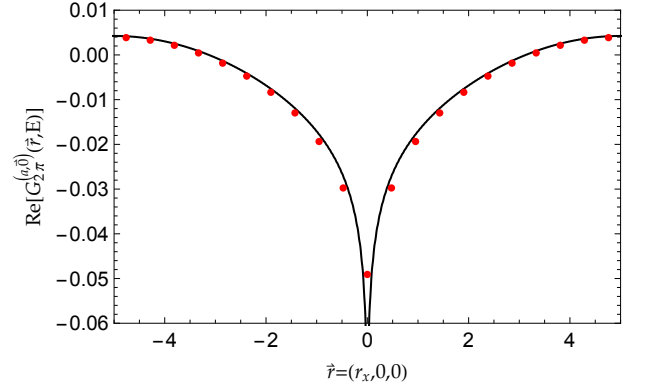


FIG. 5: Plot of real part of finite spacing version of $G_{2\pi}^{(a,0)}(\mathbf{r}; E) = \sum_{\mathbf{p}} e^{i\mathbf{p}\cdot\mathbf{r}} \tilde{G}_{2\pi}^{(a,0)}(\mathbf{p}; E)$ (red dots) compared with its infinite volume counterpart (black curve) with chosen parameters: $\mathbf{r} = (r_x, 0, 0)$, $E = 1\text{GeV}$, $L = 10\text{GeV}^{-1}$, $m_\pi = 0.200\text{GeV}$, and $a = 0.48\text{GeV}^{-1}$.

ing is obtained by replacing Eq.(6) by

$$\begin{aligned} t_{2\pi}^{(a,\mathbf{P})}(\mathbf{k}) &= \sum_{\mathbf{p}} \tilde{V}(|\mathbf{k} - \mathbf{p}|) \tilde{G}_{2\pi}^{(a,\mathbf{P})}(\mathbf{p}; E) t_{2\pi}^{(a,\mathbf{P})}(\mathbf{p}), \\ (\mathbf{k}, \mathbf{p}) &\in \frac{2\pi\mathbf{n}}{L}, \quad (n_x, n_y, n_z) \in [-N, N]. \quad (51) \end{aligned}$$

For contact interaction, a finite lattice spacing may play the role of natural ultraviolet cutoff, Eq.(34) is thus replaced by

$$\frac{1}{V_R(\mu)} = \sum_{\mathbf{p}} \tilde{G}_{2\pi}^{(a,\mathbf{P})}(\mathbf{p}; E) - \sum_{\mathbf{p}} \tilde{G}_{2\pi}^{(a,0)}(\mathbf{p}; \mu), \quad (52)$$

where sum of $\mathbf{p} = \frac{2\pi\mathbf{n}}{L}$ is restricted in first Brillouin zone with $(n_x, n_y, n_z) \in [-N, N]$ and $N = \frac{L}{2a} - 1$.

2. $3\pi^+$ LS equation with finite lattice spacing

With same strategy, the finite lattice spacing version of $3\pi^+$ LS equation is obtained by replacing Eq.(43) by

$$\begin{aligned} t_{3\pi}^{(a,\mathbf{P})}(\mathbf{k}) &= 2 \sum_{\mathbf{p}} \frac{4 \sinh \frac{aE_{\mathbf{p}}}{2} \frac{L^3}{a} \tilde{G}_{3\pi}^{(a,\mathbf{P})}(\mathbf{p}, \mathbf{k}; E)}{\frac{1}{V_R(\mu)} - \tilde{S}_{3\pi}^{(a,\mathbf{P})}(\mathbf{k}; E, \mu)} t_{3\pi}^{(a,\mathbf{P})}(\mathbf{p}), \\ (\mathbf{k}, \mathbf{p}) &\in \frac{2\pi\mathbf{n}}{L}, \quad (n_x, n_y, n_z) \in [-N, N], \quad (53) \end{aligned}$$

where

$$\begin{aligned} \tilde{S}_{3\pi}^{(a,\mathbf{P})}(\mathbf{k}; E, \mu) &= \sum_{\mathbf{p}} \left[4 \sinh \frac{aE_{\mathbf{k}}}{2} \frac{L^3}{a} \tilde{G}_{3\pi}^{(a,\mathbf{P})}(\mathbf{p}, \mathbf{k}; E) - \tilde{G}_{2\pi}^{(a,0)}(\mathbf{p}; \mu) \right], \quad (54) \end{aligned}$$

and $\mathbf{p} = \frac{2\pi\mathbf{n}}{L}$, $(n_x, n_y, n_z) \in [-N, N]$.

B. Cubic lattice symmetry group and its irreducible representations

The energy spectrum of a quantum system is normally organized and labeled according to irreducible representations (irreps) of the symmetry groups of the system. These irreps carry so-called “good” quantum numbers that help in practice identify states of the system. For example, in infinite volume, hadronic bound states are typically labeled in terms of total angular momentum and parity based on the system’s behavior under rotations and space inversion. To decouple states with different quantum numbers, one can project the dynamic equations of the system onto each irrep of symmetry groups. The end result is that each eigen-energy belongs to certain irrep, or irreps in the case of degeneracy.

Similar operations can be carried out for finite-volume systems as well. The energy spectra of finite-volume multi- π^+ system are expected to be labeled by irreps of the cubic lattice symmetry group. For instance, the cubic symmetry group for a system with vanishing total momentum, $\mathbf{P} = 0$, is the octahedral group O_h , which consists of 48 symmetry operations, including 24 discrete space rotations and inversions of all axes. The irreps of octahedral group O_h include one-dimensional representations, A_1^\pm and A_2^\pm , two-dimensional representation, E^\pm , and three-dimensional representations, T_1^\pm and T_2^\pm . The superscripts \pm are used to label even or odd parity state of the system. A brief introduction on the subject of irrep projection of dynamical equations is given in this section, with the $2\pi^+$ LS equation used as a specific example. More elaborate explanations on the subject can be found in, e.g., Refs. [54, 78]. The irrep-projected $2\pi^+$ and $3\pi^+$ LS equations in the CM frame will be presented in the following subsections.

We start with the projection operator for the cubic group [78],

$$\mathcal{P}_{\alpha,\alpha}^{(\lambda)} = \frac{d_\lambda}{48} \sum_{g \in \mathcal{G}} \Gamma_{\alpha,\alpha}^{(\lambda)*}(g) \mathbf{O}(g), \quad (55)$$

where \mathcal{G} and g stand for the the cubic symmetry group and its elements. Here λ is used to label a specific irrep, and d_λ denotes the dimension of irrep λ , e.g., $d_\lambda = 1, 1, 2, 3, 3$ for $\lambda = A_1^\pm, A_2^\pm, E^\pm, T_1^\pm, T_2^\pm$, respectively. With g running over all elements of \mathcal{G} , $\Gamma^{(\lambda)}(g)$ are a set of d_λ -by- d_λ matrices that furnish irrep λ . $\mathbf{O}(g)$ represents the symmetry operation implemented on quantum states. These operations are perhaps most easily explained by their action on momenta or coordinates of the particles. For instance,

$$\mathbf{p}' = \mathbf{O}(g)\mathbf{p} = g\mathbf{p},$$

where $|\mathbf{p}'| = |\mathbf{p}|$ for all $g \in \mathcal{G}$, because operations in O_h are either rotation or inversion. The complete list of symmetry operations of the octahedral group O_h are given in Appendix C.

Momenta of a particle can be grouped into various sets, and momenta in the same set are connected by symmetry operations. Any set of such momenta can be represented by a single reference vector \mathbf{p}_0 , and the rest of members of this particular set can be reached by

$$\mathbf{p} = g\mathbf{p}_0 \quad (g \in \mathcal{G}).$$

The reference vector used in this work is the same concept as used in Ref. [54], while in Ref. [78] the set of momenta represented by \mathbf{p}_0 is called the “star” of \mathbf{p}_0 . With a cutoff on the lattice momenta,

$$\mathbf{p} = \frac{2\pi\mathbf{n}}{L}, \quad (n_x, n_y, n_z) \in [-N, N],$$

the reference vectors, \mathbf{p}_0 ’s, may be chosen as

$$\mathbf{p}_0 \in \left\{ \frac{2\pi}{L} \mathbf{n}_{i,j,k} \right\},$$

where

$$\mathbf{n}_{i,j,k} = (k, j, i),$$

and $(i, j, k) \in [0, N]$ satisfies $k \leq j \leq i$. The total number of reference vectors \mathbf{p}_0 for a fixed N is thus given by

$$\sum_{i=0}^N \sum_{j=0}^i \sum_{k=0}^j = \frac{1}{6}(N+1)(N+2)(N+3).$$

In terms of reference vectors and symmetry operations, the sum of momenta over an arbitrary function can be reorganized as follows:

$$\sum_{\mathbf{p}} f(\mathbf{p}) = \sum_{\mathbf{p}_0} \frac{\vartheta(\mathbf{p}_0)}{48} \sum_{g \in \mathcal{G}} f(g\mathbf{p}_0), \quad (56)$$

where $\vartheta(\mathbf{p}_0)$ is the multiplicity of distinct momenta within the set represented by \mathbf{p}_0 . For instance, for

$$\mathbf{p}_0 = \frac{2\pi}{L}(0, 0, 1),$$

$\vartheta(\mathbf{p}_0) = 6$ and the six distinct momenta are

$$\mathbf{p} = g\mathbf{p}_0 \in \frac{2\pi}{L} \{(0, 0, \pm 1), (0, \pm 1, 0), (\pm 1, 0, 0)\}.$$

The multiplicity function $\vartheta(\mathbf{p}_0)$ used in this work has the same meaning as the multiplicity of a given shell defined in Ref. [54]. Therefore, the projector defined in Eq.(55) acting on amplitudes can be interpreted as weighted average within the momentum set represented by \mathbf{p}_0 , and the projected amplitudes can be labeled by \mathbf{p}_0 ’s.

C. Irrep projection of $2\pi^+$ LS equation

As an example, we discuss projection of two-pion amplitudes for $\mathbf{P} = \mathbf{0}$ onto irrep λ that is given by

$$t_{2\pi}^{(\lambda)}(\mathbf{k}_0) = \mathcal{P}_{\alpha,\alpha}^{(\lambda)} t_{2\pi}^{(\mathbf{0})}(\mathbf{k}) = \frac{d_\lambda}{48} \sum_{g \in \mathcal{G}} \Gamma_{\alpha,\alpha}^{(\lambda)*}(g) t_{2\pi}^{(\mathbf{0})}(g\mathbf{k}_0). \quad (57)$$

The projected amplitude, $t_{2\pi}^{(\lambda)}(\mathbf{k}_0)$, actually does not depend on quantum number α due to the cubic symmetry of the system. Therefore, it may be convenient to express the projection operator in terms of the character of irreps:

$$\mathcal{P}^{(\lambda)} = \frac{1}{d_\lambda} \sum_{\alpha} \mathcal{P}_{\alpha,\alpha}^{(\lambda)} = \frac{1}{48} \sum_{g \in \mathcal{G}} \chi^{(\lambda)*}(g) \mathbf{O}(g), \quad (58)$$

where

$$\chi^{(\lambda)}(g) = \sum_{\alpha} \Gamma_{\alpha,\alpha}^{(\lambda)}(g)$$

is the character of irrep λ , and it satisfies orthogonality relation:

$$\frac{1}{48} \sum_{g \in \mathcal{G}} \chi^{(\lambda)*}(g) \chi^{(\lambda')}(g) = \delta_{\lambda,\lambda'}. \quad (59)$$

With the help of $\mathcal{P}^{(\lambda)}$, one can rewrite the projection of two-pion amplitudes in a more compact form:

$$t_{2\pi}^{(\lambda)}(\mathbf{k}_0) = \frac{1}{48} \sum_{g \in \mathcal{G}} \chi^{(\lambda)*}(g) t_{2\pi}^{(0)}(g\mathbf{k}_0). \quad (60)$$

The above equation can be inverted using the orthogonality relation:

$$t_{2\pi}^{(0)}(g\mathbf{k}_0) = \sum_{\lambda} \chi^{(\lambda)}(g) t_{2\pi}^{(\lambda)}(\mathbf{k}_0). \quad (61)$$

Projection of dynamic equations established in previous sections is obtained by applying projection formula of amplitudes. Applying Eqs. (60), (61), and (56) to Eq. (6), we arrive at

$$t_{2\pi}^{(\lambda)}(\mathbf{k}_0) = \sum_{\mathbf{p}_0} \vartheta(\mathbf{p}_0) \tilde{V}^{(\lambda)}(\mathbf{k}_0, \mathbf{p}_0) \tilde{G}_{2\pi}^{(0)}(\mathbf{p}_0; E) t_{2\pi}^{(\lambda)}(\mathbf{p}_0), \quad (62)$$

where $\tilde{V}^{(\lambda)}(\mathbf{k}_0, \mathbf{p}_0)$ is the projected potential:

$$\begin{aligned} & \delta_{\lambda,\lambda'} \tilde{V}^{(\lambda)}(\mathbf{k}_0, \mathbf{p}_0) \\ &= \frac{1}{48^2} \sum_{g_{\mathbf{p}}, g_{\mathbf{k}} \in \mathcal{G}} \chi^{(\lambda)*}(g_{\mathbf{k}}) \tilde{V}(|g_{\mathbf{k}}\mathbf{k}_0 - g_{\mathbf{p}}\mathbf{p}_0|) \chi^{(\lambda')}(g_{\mathbf{p}}) \\ &= \delta_{\lambda,\lambda'} \frac{1}{48} \sum_{g \in \mathcal{G}} \chi^{(\lambda)*}(g) \tilde{V}(|g\mathbf{k}_0 - \mathbf{p}_0|). \end{aligned} \quad (63)$$

The energy spectrum stemming from the irrep-projected dynamical equation is of course labeled by the same irrep.

With the contact interaction, $\tilde{V}(k) = V_0$, only A_1^+ irrep survives after projection of the potential:

$$\tilde{V}^{(\lambda)}(\mathbf{k}_0, \mathbf{p}_0) = \delta_{\lambda, A_1^+} V_0.$$

Therefore, projection of Eq.(52) yields non-trivial solutions only in A_1^+ :

$$\frac{\delta_{\lambda, A_1^+}}{V_R(\mu)} = \sum_{\mathbf{p}_0} \vartheta(\mathbf{p}_0) \tilde{G}_{2\pi}^{(a,0)}(\mathbf{p}_0; E) - \sum_{\mathbf{p}_0} \vartheta(\mathbf{p}_0) \tilde{G}_{2\pi}^{(a,0)}(\mathbf{p}_0; \mu). \quad (64)$$

D. Irrep projection of $3\pi^+$ LS equation

Since the three-pion amplitudes depend on two momentum variables, the irrep projection can be done by first projecting out each momentum dependence separately onto the corresponding irrep, and then coupling two individual projections to an irrep of the $3\pi^+$ system. This procedure resembles addition of angular momenta, which is essentially reduction of tensor product of two $SO(3)$ irreps.

Following that idea, projection of $3\pi^+$ amplitude $t_{(k)}^{(0)}(\mathbf{k}_1, \mathbf{k}_2)$ is accomplished by the following operator:

$$\mathcal{P}_{\alpha}^{(\lambda)}(1, 2) = \sum_{\alpha_1, \alpha_2} \left(\begin{array}{cc|c} \lambda_1 & \lambda_2 & \lambda \\ \alpha_1 & \alpha_2 & \alpha \end{array} \right) \mathcal{P}_{\alpha_1, \alpha_1}^{(\lambda_1)}(1) \mathcal{P}_{\alpha_2, \alpha_2}^{(\lambda_2)}(2), \quad (65)$$

where $\mathcal{P}_{\alpha_1, \alpha_1}^{(\lambda_1)}(1)$ and $\mathcal{P}_{\alpha_2, \alpha_2}^{(\lambda_2)}(2)$ are the uncoupled irrep projection operators on momenta \mathbf{k}_1 and \mathbf{k}_2 , respectively, and

$$\left(\begin{array}{cc|c} \lambda_1 & \lambda_2 & \lambda \\ \alpha_1 & \alpha_2 & \alpha \end{array} \right)$$

is the Clebsch-Gordan coefficient that couple irreps λ_1 and λ_2 to irrep λ on the α -th row. Again, due to the cubic symmetry of the system, projected three-body amplitudes do not depend on α , so the projection of $t_{(k)}^{(0)}(\mathbf{k}_1, \mathbf{k}_2)$ can be written as

$$\begin{aligned} t_{(k)}^{(\lambda)}(\mathbf{k}_{10}, \mathbf{k}_{20}) &= \frac{1}{d_\lambda} \sum_{\alpha} \mathcal{P}_{\alpha}^{(\lambda)}(1, 2) t_{(k)}^{(0)}(\mathbf{k}_1, \mathbf{k}_2) \\ &= \frac{d_{\lambda_1} d_{\lambda_2}}{48^2} \frac{1}{d_\lambda} \sum_{\alpha_1, \alpha_2, \alpha} \left(\begin{array}{cc|c} \lambda_1 & \lambda_2 & \lambda \\ \alpha_1 & \alpha_2 & \alpha \end{array} \right) \\ &\quad \times \sum_{g_1, g_2 \in \mathcal{G}} \Gamma_{\alpha_1, \alpha_1}^{(\lambda_1)*}(g_1) \Gamma_{\alpha_2, \alpha_2}^{(\lambda_2)*}(g_2) t_{(k)}^{(0)}(g_1 \mathbf{k}_{10}, g_2 \mathbf{k}_{20}). \end{aligned} \quad (66)$$

The general projection of three-particle amplitudes can be cumbersome. However for the interaction under consideration in the present paper, no three-body force and only pair-wise contact interaction, the procedure is greatly simplified. This is because, as shown in Sec. II C, the three-pion amplitude depends only on a single momentum: $t_{3\pi}^{(\mathbf{P})}(\mathbf{k}_2)$. With no dependence on \mathbf{k}_1 , only the trivial irrep A_1^+ survives after projection of \mathbf{k}_1 dependence: $\lambda_1 = A_1^+$ and $\Gamma_{\alpha_1, \alpha_1}^{(\lambda_1)} = 1$. The coupled irrep of the $3\pi^+$ system is thus determined by \mathbf{k}_2 dependence alone: $\lambda = \lambda_2$ and $\alpha = \alpha_2$. Therefore, one can apply straightforwardly most of the results for the two-pion case in Sec. III C to the irrep projection of the $3\pi^+$ LS equation.

With pair-wise contact interaction, the irrep projection of $t_{3\pi}^{(0)}(\mathbf{k}_2)$ in the CM frame is given by

$$t_{3\pi}^{(\lambda)}(\mathbf{k}_0) = \frac{1}{48} \sum_{g \in \mathcal{G}} \chi^{(\lambda)*}(g) t_{3\pi}^{(a,0)}(g\mathbf{k}_0). \quad (67)$$

Similar to Eq.(61), we also have

$$t_{3\pi}^{(a,0)}(g\mathbf{k}_0) = \sum_{\lambda} \chi^{(\lambda)}(g)t_{3\pi}^{(\lambda)}(\mathbf{k}_0). \quad (68)$$

Noticing that $\tilde{S}_{3\pi}^{(a,0)}(\mathbf{k}_0; E, \mu)$ remains invariant under symmetry operations,

$$\tilde{S}_{3\pi}^{(a,0)}(g\mathbf{k}_0; E, \mu) = \tilde{S}_{3\pi}^{(a,0)}(\mathbf{k}_0; E, \mu), \quad (69)$$

and that the projection on the right-hand side of Eq.(53) yields

$$\begin{aligned} & \frac{1}{48^2} \sum_{g_1, g_2 \in \mathcal{G}} \chi^{(\lambda)*}(g_1)\chi^{(\lambda')}(g_2) \\ & \times \left[4 \sinh \frac{aE_{g_2\mathbf{p}_0}}{2} \frac{L^3}{a} \tilde{G}_{3\pi}^{(a,0)}(g_2\mathbf{p}_0, g_1\mathbf{k}_0; E) \right] \\ & = \delta_{\lambda, \lambda'} \frac{1}{48} \sum_{g \in \mathcal{G}} \chi^{(\lambda)*}(g) 4 \sinh \frac{aE_{\mathbf{p}_0}}{2} \frac{L^3}{a} \tilde{G}_{3\pi}^{(a,0)}(\mathbf{p}_0, g\mathbf{k}_0; E), \end{aligned} \quad (70)$$

one can show that irrep projection of the $3\pi^+$ LS equation (53) ultimately leads to the following:

$$t_{3\pi}^{(\lambda)}(\mathbf{k}_0) = 2 \sum_{\mathbf{p}_0} \frac{\vartheta(\mathbf{p}_0) \tilde{C}_{3\pi}^{(\lambda)}(\mathbf{k}_0, \mathbf{p}_0; E)}{\frac{1}{V_R(\mu)} - \tilde{S}_{3\pi}^{(a,0)}(\mathbf{k}_0; E, \mu)} t_{3\pi}^{(\lambda)}(\mathbf{p}_0), \quad (71)$$

where

$$\begin{aligned} & \tilde{C}_{3\pi}^{(\lambda)}(\mathbf{k}_0, \mathbf{p}_0; E) \\ & = \frac{1}{48} \sum_{g \in \mathcal{G}} \chi^{(\lambda)*}(g) 4 \sinh \frac{aE_{\mathbf{p}_0}}{2} \frac{L^3}{a} \tilde{G}_{3\pi}^{(a,0)}(\mathbf{p}_0, g\mathbf{k}_0; E). \end{aligned} \quad (72)$$

The O_h -irrep projected $3\pi^+$ quantization condition, under our assumptions, has a simple form:

$$\det \left[\delta_{\mathbf{k}_0, \mathbf{p}_0} - \frac{2\vartheta(\mathbf{p}_0) \tilde{C}_{3\pi}^{(\lambda)}(\mathbf{k}_0, \mathbf{p}_0; E)}{\frac{1}{V_R(\mu)} - \tilde{S}_{3\pi}^{(a,0)}(\mathbf{k}_0; E, \mu)} \right] = 0. \quad (73)$$

The above equation suggests that except for A_1^+ irrep, only trivial solutions — free particle states — can be found near the ground state with all three pions at rest, because the only irrep in which $\tilde{C}_{3\pi}^{(\lambda)}(\mathbf{0}, \mathbf{0}; E)$ does not vanish is $\lambda = A_1^+$.

IV. NUMERICAL RESULTS

In this section, we use the quantization conditions (64) and (73) to produce $2\pi^+$ and $3\pi^+$ energy spectra for various lattice sizes. A single parameter, the renormalized coupling of the two-body contact interaction $V_R(\mu)$, is fitted to the lattice results of Ref. [27].

The two-pion scattering parameters, the scattering length a_0 and effective range r_0 , can immediately be produced once $V_R(\mu)$ is determined from the fit. a_0 and r_0 are usually defined by the effective range expansion at low energies:

$$p \cot \delta(E) = -\frac{1}{a_0} + \frac{r_0}{2} p^2 + \mathcal{O}(p^4), \quad (74)$$

where

$$p = \frac{1}{2} \sqrt{E^2 - 4m_\pi^2}$$

is relative momentum of the pions in the CM frame. On the other hand, as detailed in Appendix B, the isospin-2 S -wave phase shift of $\pi^+\pi^+$ scattering through a pair-wise contact potential is given by

$$\cot \delta_0^{(2)}(E) = -\frac{16\pi}{\sqrt{1 - \frac{4m_\pi^2}{E^2}}} \left[\frac{1}{V_R(\mu)} - \text{Re}G(E) + G(\mu) \right], \quad (75)$$

where

$$G(E) = \frac{\sqrt{1 - \frac{4m_\pi^2}{E^2}}}{16\pi^2} \ln \frac{\sqrt{1 - \frac{4m_\pi^2}{\mu^2}} + 1}{\sqrt{1 - \frac{4m_\pi^2}{E^2}} - 1}.$$

Comparing Eqs. (74) and (75), one finds a_0 and r_0 in terms of $V_R(\mu)$:

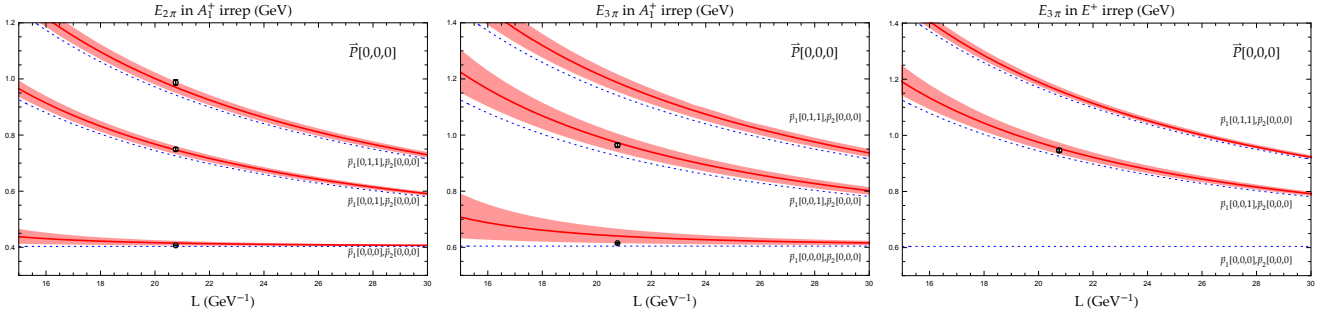
$$\begin{aligned} \frac{1}{a_0 m_\pi} &= 16\pi \left[\frac{1}{V_R(\mu)} + G(\mu) \right], \\ r_0 m_\pi &= \frac{1}{a_0 m_\pi} + \frac{4}{\pi}. \end{aligned} \quad (76)$$

The values of $\pi^+\pi^+$ scattering length a_0 and effective range r_0 extracted in this study are compared in Table I with the values given by other works. Using Eq.(75), the $\pi^+\pi^+$ S -wave phase shifts are plotted in Fig. 7.

Treating $V_R(\mu)$ as a free parameter, one can produce the CM-frame $2\pi^+$ and $3\pi^+$ energy spectra in A_1^+ and E^+ irreps with Eqs. (64) and (73), at lattice spacing $a = 0.324\text{GeV}^{-1}$ and pion mass $m_\pi = 0.2\text{GeV}$. The spectra are then matched to the lattice results reported in Ref. [27], as shown in Fig. 6. The renormalization scale is chosen at $\mu = 0\text{GeV}$, so that $G(\mu) = \frac{1}{8\pi^2}$ is real. The value of coupling constant of contact interaction is extracted,

$$V_R(0) \sim 17.5 \pm 12.5. \quad (77)$$

As illustrated in Fig. 6, with only one parameter, Eqs. (64) and (64) struggle to match the lattice results, so the fit yields a large error on the value of $V_R(0)$. This suggests that more sophisticated pair-wise interactions and/or three-body interactions may be needed.



(a) $2\pi^+$ energy spectrum in A_1^+ irrep. (b) $3\pi^+$ energy spectrum in A_1^+ irrep. (c) $3\pi^+$ energy spectrum in E^+ irrep.

FIG. 6: $2\pi^+$ and $3\pi^+$ energy spectrum in irreps A_1^+ and E^+ and CM frame: red bands are spectrum produced by using Eq.(64) and Eq.(73) for $2\pi^+$ and $3\pi^+$ respectively, the lattice results (black circles) are taken from [27]. The free multi- π^+ energy spectrum (blue dashed curves) by using $E = \frac{2}{a} \sinh^{-1}(\sum_i \sinh \frac{aE_{\mathbf{p}_i}}{2})$ and $\sum_i \mathbf{p}_i = \mathbf{P}$ are also plotted as reference. The lattice spacing used in this work and in [27] is $a = 0.324\text{GeV}^{-1}$, $m_\pi = 0.200\text{GeV}$.

TABLE I: $\pi^+\pi^+$ scattering length a_0 and effective range r_0 .

	$a_0 m_\pi$	$r_0 m_\pi$	m_π (GeV)
This work	0.28 ± 0.17	4.8 ± 2.1	0.200
Lattice in [27]	0.1019 ± 0.0088	9.0 ± 2.4	0.200
Lattice in [20]	0.307 ± 0.013	-0.26 ± 0.13	0.396
Analysis in [62]	0.090 ± 0.006	28.78 ± 0.89	0.200

tic $2\pi^+$ and $3\pi^+$ dynamics in finite volume are presented in the paper. The presentation of multi- π^+ dynamics included both pair-wise and three-body interactions, and the effects of finite lattice spacing and projections onto irreps of the cubic lattice group were also discussed. The quantization conditions were used to analyze the lattice data published in [27]. In the present work, only contact pair-wise interactions were employed in our analysis and, as a result, the renormalized coupling strength was the sole free parameter. The scattering length a_0 and effective range r_0 were obtained, however, with rather large uncertainty: $a_0 m_\pi = 0.28 \pm 0.17$ and $r_0 m_\pi = 4.8 \pm 2.1$, which might be attributed to the lack of accuracy in describing long-range interactions among the π^+ 's by only a contact pair-wise interaction. It may also suggest that it is worth investigating the role of three-pion forces.

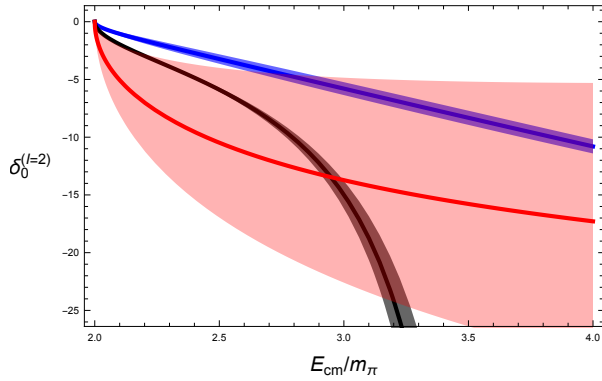


FIG. 7: Phase shift $\delta_0^{(I=2)}(E)$ by using Eq.(75) (red band) compared with the phase shift given by effective range expansion formula (black band), Eq.(74), where $a_0 m_\pi = 0.1019 \pm 0.0088$ and $r_0 m_\pi = 9.0 \pm 2.4$ are taken from [27]. For the reference, the physical phase shift by using parameterization given in [79] is also plotted (blue band).

V. SUMMARY

Based on the variational approach combined with the Faddeev method proposed in Refs. [64–67], the relativis-

ACKNOWLEDGMENTS

We acknowledge support from the Department of Physics and Engineering, California State University, Bakersfield, CA. This research was supported in part by the National Science Foundation under Grant No. NSF PHY-1748958. P.G. acknowledges GPU computing resources (<http://complab.cs.csuak.edu>) from the Department of Computer and Electrical Engineering and Computer Science at California State University-Bakersfield made available for conducting the research reported in this work. B.L. acknowledges support by the National Science Foundation of China under Grant Nos.11775148 and 11735003.

Appendix A: Reduction of Bethe-Salpeter equation to relativistic $3\pi^+$ Lippmann-Schwinger equation

Consider the general form of Bethe-Salpeter (BS) equation [80] for three-scalar-particle bound states:

$$\psi_{BS}(p_1, p_2) = \frac{(-i)^2}{(p_1^2 - m_\pi^2)(p_2^2 - m_\pi^2)(p_3^2 - m_\pi^2)} \times \int \frac{d^4 p'_1}{(2\pi)^4} \frac{d^4 p'_2}{(2\pi)^4} I(p'_1 - p_1, p'_2 - p_2) \psi_{BS}(p'_1, p'_2), \quad (\text{A1})$$

where $p_i = (p_{i0}, \mathbf{p}_i)$ are the four momenta of three particles, the three-body BS wave function is labeled only by two independent particle momenta, p_1 and p_2 , since the momenta of three particles are constrained by energy-momentum conservation, $p_3 = P - p_1 - p_2$. Assuming "instantaneous interaction kernel", $I(p_1, p_2) = I(\mathbf{p}_1, \mathbf{p}_2)$, and introducing Lippmann-Schwinger equation wave function, $\psi(\mathbf{p}_1, \mathbf{p}_2) = \int \frac{dp_{10}}{2\pi} \frac{dp_{20}}{2\pi} \psi_{BS}(p_1, p_2)$, hence, we get

$$\psi(\mathbf{p}_1, \mathbf{p}_2) = \int \frac{dp_{10}}{2\pi} \frac{dp_{20}}{2\pi} \frac{(-i)^2}{(p_1^2 - m_\pi^2)(p_2^2 - m_\pi^2)(p_3^2 - m_\pi^2)} \times \int \frac{d\mathbf{p}'_1}{(2\pi)^3} \frac{d\mathbf{p}'_2}{(2\pi)^3} I(\mathbf{p}'_1 - \mathbf{p}_1, \mathbf{p}'_2 - \mathbf{p}_2) \psi(\mathbf{p}'_1, \mathbf{p}'_2). \quad (\text{A2})$$

The integration over propagators can be carried out,

$$(2\pi)^6 G^{(\mathbf{P})}(\mathbf{p}_1, \mathbf{p}_2; E) = \int \frac{dp_{10}}{2\pi} \frac{dp_{20}}{2\pi} \frac{(-i)^2}{(p_1^2 - m_\pi^2)(p_2^2 - m_\pi^2)(p_3^2 - m_\pi^2)} = \frac{1}{2E_{\mathbf{p}_1} 2E_{\mathbf{p}_2} 2E_{\mathbf{p}_3}} \frac{2(E_{\mathbf{p}_1} + E_{\mathbf{p}_2} + E_{\mathbf{p}_3})}{E^2 - (E_{\mathbf{p}_1} + E_{\mathbf{p}_2} + E_{\mathbf{p}_3})^2}, \quad (\text{A3})$$

where $E_{\mathbf{p}_i} = \sqrt{\mathbf{p}_i^2 + m_\pi^2}$.

The interactions of $3\pi^+$ consist of pair-wise interactions and three-body interaction potential,

$$I(\mathbf{p}'_1 - \mathbf{p}_1, \mathbf{p}'_2 - \mathbf{p}_2) = \tilde{V}_{(4)}(\mathbf{p}'_1 - \mathbf{p}_1, \mathbf{p}'_2 - \mathbf{p}_2) + \sum_{k=1}^3 2E_{\mathbf{p}_k} (2\pi)^3 \delta(\mathbf{p}'_k - \mathbf{p}_k) \tilde{V}(|\mathbf{q}'_{ij} - \mathbf{q}_{ij}|) |_{k \neq i \neq j}, \quad (\text{A4})$$

where symbols \tilde{V} and $\tilde{V}_{(4)}$ are used to denote pair-wise interaction and three-body force respectively in consistent with the conventions used in Section II. $\mathbf{q}_{ij} = \frac{\mathbf{p}_i - \mathbf{p}_j}{2}$ refers to the relative momentum between i -th and j -th pions. The relativistic kinematic factors $\langle \mathbf{p}_k | \mathbf{p}'_k \rangle = 2E_{\mathbf{p}_k} (2\pi)^3 \delta(\mathbf{p}'_k - \mathbf{p}_k)$ emerge when k -th particle is free propagating and not involved in the interaction. The relativistic $3\pi^+$ Lippmann-Schwinger equation is thus given

explicitly by

$$\psi(\mathbf{p}_1, \mathbf{p}_2) = G^{(\mathbf{P})}(\mathbf{p}_1, \mathbf{p}_2; E) \times \left[2E_{\mathbf{p}_1} (2\pi)^3 \int d\mathbf{p}'_2 \tilde{V}(|\mathbf{p}'_2 - \mathbf{p}_2|) \psi(\mathbf{p}_1, \mathbf{p}'_2) + 2E_{\mathbf{p}_2} (2\pi)^3 \int d\mathbf{p}'_1 \tilde{V}(|\mathbf{p}'_1 - \mathbf{p}_1|) \psi(\mathbf{p}'_1, \mathbf{p}_2) + 2E_{\mathbf{p}_3} (2\pi)^3 \int d\mathbf{p}'_1 \tilde{V}(|\mathbf{p}'_1 - \mathbf{p}_1|) \psi(\mathbf{p}'_1, \mathbf{p}_1 + \mathbf{p}_2 - \mathbf{p}'_1) + \int d\mathbf{p}'_1 d\mathbf{p}'_2 \tilde{V}_{(4)}(\mathbf{p}'_1 - \mathbf{p}_1, \mathbf{p}'_2 - \mathbf{p}_2) \psi(\mathbf{p}'_1, \mathbf{p}'_2) \right]. \quad (\text{A5})$$

Appendix B: 2π scattering amplitude in infinite volume with contact interaction

With the contact interaction,

$$V(r) = V_0 \delta(\mathbf{r}),$$

the relativistic Lippmann-Schwinger equation of 2π system can be solved analytically, so the scattering wave function of 2π in infinite volume and in CM frame is given by

$$\phi_{\mathbf{p}}(\mathbf{r}) = e^{i\mathbf{p}\cdot\mathbf{r}} + G^{(0)}(\mathbf{r}; E) V_0 \phi_{\mathbf{p}}(\mathbf{0}), \quad (\text{B1})$$

where \mathbf{r} and \mathbf{p} are the relative coordinate and momentum of two pions respectively. The total energy of two pions is related to \mathbf{p} by $E = 2E_{\mathbf{p}} = 2\sqrt{\mathbf{p}^2 + m_\pi^2}$. The two pions Green's function in CM frame in infinite volume is given by

$$G^{(0)}(\mathbf{r}; E) = \int \frac{d\mathbf{q}}{(2\pi)^3} \frac{1}{E_{\mathbf{q}}} \frac{e^{i\mathbf{q}\cdot\mathbf{r}}}{E^2 - (2E_{\mathbf{q}})^2}. \quad (\text{B2})$$

The two pions amplitude in CM frame is thus given by,

$$t(E) = -V_0 \phi_{\mathbf{p}}(\mathbf{0}) = -\frac{1}{\frac{1}{V_0} - G^{(0)}(\mathbf{0}; E)}. \quad (\text{B3})$$

The Green's function $G^{(0)}(\mathbf{0}; E)$ diverge at $\mathbf{r} = \mathbf{0}$, a cut-off Λ on momentum integration may be introduced to regularize ultraviolet divergence, as $\Lambda \rightarrow \infty$ hence we find

$$\int^\Lambda \frac{d\mathbf{q}}{(2\pi)^3} \frac{1}{E_{\mathbf{q}}} \frac{1}{E^2 - (2E_{\mathbf{q}})^2} = G(E) - \frac{1}{8\pi^2} \ln \frac{2\Lambda}{m_\pi}, \quad (\text{B4})$$

where

$$G(E) = \frac{\sqrt{1 - \frac{4m_\pi^2}{E^2}}}{16\pi^2} \ln \frac{\sqrt{1 - \frac{4m_\pi^2}{E^2}} + 1}{\sqrt{1 - \frac{4m_\pi^2}{E^2}} - 1}. \quad (\text{B5})$$

The imaginary part of function $G(E)$ is non-zero only above threshold of two pions: $ImG(E) = -\frac{1}{16\pi} \sqrt{1 - \frac{4m_\pi^2}{E^2}}$ for $E > 2m_\pi$, and zero otherwise. The

ultraviolet divergence may be absorbed by redefining bare coupling, V_0 ,

$$\frac{1}{V_0} = \frac{1}{V_R(\mu)} + G(\mu) - \frac{1}{8\pi^2} \ln \frac{2\Lambda}{m_\pi}, \quad (\text{B6})$$

where $V_R(\mu)$ stands for the renormalized coupling strength at a renormalization scale μ . μ will be chosen below two pions threshold, so that $G(\mu)$ is real. Therefore, the cutoff dependence is cancelled out completely, and renormalized scattering amplitude is now given by

$$t(E) = -\frac{1}{\frac{1}{V_R(\mu)} - G(E) + G(\mu)}, \quad \mu < 2m_\pi. \quad (\text{B7})$$

The phase shift is defined by $t(E) = \frac{16\pi}{\sqrt{1 - \frac{4m_\pi^2}{E^2}}} \frac{1}{\cot \delta(E) - i}$,

hence we obtain

$$\cot \delta(E) = -\frac{16\pi}{\sqrt{1 - \frac{4m_\pi^2}{E^2}}} \left[\frac{1}{V_R(\mu)} - \text{Re}G(E) + G(\mu) \right]. \quad (\text{B8})$$

Expanding phase shift near threshold $p = |\mathbf{p}| = \frac{1}{2}\sqrt{E^2 - 4m_\pi^2} \sim 0$, we find

$$p \cot \delta(E) = -\frac{1}{a_0} + \frac{r_0}{2}p^2 + \mathcal{O}(p^4), \quad (\text{B9})$$

where the effective expansion parameters, a_0 and r_0 are given by

$$\begin{aligned} \frac{1}{a_0 m_\pi} &= 16\pi \left[\frac{1}{V_R(\mu)} + G(\mu) \right], \\ r_0 m_\pi &= 16\pi \left[\frac{1}{V_R(\mu)} + G(\mu) \right] + \frac{4}{\pi}. \end{aligned} \quad (\text{B10})$$

Appendix C: Character Table for the octahedral group O_h

The octahedral group O_h is the direct product of proper rotational group O that rotates a cube into itself and spatial inversion I :

$$O_h = O \times I.$$

O_h contains 48 elements, including 24 elements of rotational group O and 24 elements of combined operation of inversion and rotations: Ig where $g \in O$. The matrix representations of 24 proper rotational group O are given by

$$\begin{aligned} E &= \begin{bmatrix} 1 & 0 & 0 \\ 0 & 1 & 0 \\ 0 & 0 & 1 \end{bmatrix}, & C_{2x} &= \begin{bmatrix} 1 & 0 & 0 \\ 0 & -1 & 0 \\ 0 & 0 & -1 \end{bmatrix}, & C_{2y} &= \begin{bmatrix} -1 & 0 & 0 \\ 0 & 1 & 0 \\ 0 & 0 & -1 \end{bmatrix}, & C_{2z} &= \begin{bmatrix} -1 & 0 & 0 \\ 0 & -1 & 0 \\ 0 & 0 & 1 \end{bmatrix}, \\ C_{4x} &= \begin{bmatrix} 1 & 0 & 0 \\ 0 & 0 & 1 \\ 0 & -1 & 0 \end{bmatrix}, & C_{4y} &= \begin{bmatrix} 0 & 0 & -1 \\ 0 & 1 & 0 \\ 1 & 0 & 0 \end{bmatrix}, & C_{4z} &= \begin{bmatrix} 0 & 1 & 0 \\ -1 & 0 & 0 \\ 0 & 0 & 1 \end{bmatrix}, & C_{4x}^{-1} &= \begin{bmatrix} 1 & 0 & 0 \\ 0 & 0 & -1 \\ 0 & 1 & 0 \end{bmatrix}, \\ C_{4y}^{-1} &= \begin{bmatrix} 0 & 0 & 1 \\ 0 & 1 & 0 \\ -1 & 0 & 0 \end{bmatrix}, & C_{4z}^{-1} &= \begin{bmatrix} 0 & -1 & 0 \\ 1 & 0 & 0 \\ 0 & 0 & 1 \end{bmatrix}, & C_{2a} &= \begin{bmatrix} 0 & 1 & 0 \\ 1 & 0 & 0 \\ 0 & 0 & -1 \end{bmatrix}, & C_{2b} &= \begin{bmatrix} 0 & -1 & 0 \\ -1 & 0 & 0 \\ 0 & 0 & -1 \end{bmatrix}, \\ C_{2c} &= \begin{bmatrix} 0 & 0 & 1 \\ 0 & -1 & 0 \\ 1 & 0 & 0 \end{bmatrix}, & C_{2d} &= \begin{bmatrix} 0 & 0 & -1 \\ 0 & -1 & 0 \\ -1 & 0 & 0 \end{bmatrix}, & C_{2e} &= \begin{bmatrix} -1 & 0 & 0 \\ 0 & 0 & 1 \\ 0 & 1 & 0 \end{bmatrix}, & C_{2f} &= \begin{bmatrix} -1 & 0 & 0 \\ 0 & 0 & -1 \\ 0 & -1 & 0 \end{bmatrix}, \\ C_{3\alpha} &= \begin{bmatrix} 0 & 1 & 0 \\ 0 & 0 & -1 \\ -1 & 0 & 0 \end{bmatrix}, & C_{3\beta} &= \begin{bmatrix} 0 & -1 & 0 \\ 0 & 0 & -1 \\ 1 & 0 & 0 \end{bmatrix}, & C_{3\gamma} &= \begin{bmatrix} 0 & -1 & 0 \\ 0 & 0 & 1 \\ -1 & 0 & 0 \end{bmatrix}, & C_{3\delta} &= \begin{bmatrix} 0 & 1 & 0 \\ 0 & 0 & 1 \\ 1 & 0 & 0 \end{bmatrix}, \\ C_{3\alpha}^{-1} &= \begin{bmatrix} 0 & 0 & -1 \\ 1 & 0 & 0 \\ 0 & -1 & 0 \end{bmatrix}, & C_{3\beta}^{-1} &= \begin{bmatrix} 0 & 0 & 1 \\ -1 & 0 & 0 \\ 0 & -1 & 0 \end{bmatrix}, & C_{3\gamma}^{-1} &= \begin{bmatrix} 0 & 0 & -1 \\ -1 & 0 & 0 \\ 0 & 1 & 0 \end{bmatrix}, & C_{3\delta}^{-1} &= \begin{bmatrix} 0 & 0 & 1 \\ 1 & 0 & 0 \\ 0 & 1 & 0 \end{bmatrix}, \end{aligned} \quad (\text{C1})$$

and the inversion matrix,

$$I = \begin{bmatrix} -1 & 0 & 0 \\ 0 & -1 & 0 \\ 0 & 0 & -1 \end{bmatrix}. \quad (\text{C2})$$

All 48 elements of the octahedral group O_h are usually grouped into different conjugacy classes, and the mem-

TABLE II: Character table for irreps of the octahedral group O_h with positive parity

	$\chi(\mathcal{C}_1, \mathcal{C}_6)$	$\chi(\mathcal{C}_2, \mathcal{C}_7)$	$\chi(\mathcal{C}_3, \mathcal{C}_8)$	$\chi(\mathcal{C}_4, \mathcal{C}_9)$	$\chi(\mathcal{C}_5, \mathcal{C}_{10})$
A_1^+	1	1	1	1	1
A_2^+	1	1	1	-1	-1
E^+	2	-1	2	0	0
T_1^+	3	0	-1	1	-1
T_2^+	3	0	-1	-1	1

bers within the same conjugacy class share the same character value for a given irrep. Using the same convention as used in [78], ten classes of the octahedral group O_h are named as \mathcal{C}_i where $i = 1, \dots, 10$, they are associated with 48 elements by

$$\begin{aligned} \mathcal{C}_1 &= E, & \mathcal{C}_2 &= \left(C_{3\alpha}, C_{3\beta}, C_{3\gamma}, C_{3\delta}, \right. \\ & & & \left. C_{3\alpha}^{-1}, C_{3\beta}^{-1}, C_{3\gamma}^{-1}, C_{3\delta}^{-1} \right), \\ \mathcal{C}_3 &= (C_{2x}, C_{2y}, C_{2z}), & \mathcal{C}_4 &= \left(C_{4x}, C_{4y}, C_{4z}, \right. \\ & & & \left. C_{4x}^{-1}, C_{4y}^{-1}, C_{4z}^{-1} \right), \\ \mathcal{C}_5 &= (C_{2a}, C_{2b}, C_{2c}, C_{2d}, C_{2e}, C_{2f}), \end{aligned} \quad (\text{C3})$$

and $\mathcal{C}_i = \mathcal{IC}_{(i-5)}$ for $i = 6, \dots, 10$. The character table for all irreps of the octahedral group O_h with positive parity quantum number is given in Table II.

Appendix D: Non-relativistic three-particle dynamics in finite volume

The dynamics of three non-relativistic identical bosonic particles in finite volume is described by the

$$\begin{aligned} \left[2mE + \sum_{i=1}^3 \nabla_i^2 - \sum_{k=1}^3 U(r_{ij}) - U_{(4)}(\mathbf{r}_{13}, \mathbf{r}_{23}) \right] \\ \times \Phi(\mathbf{x}_1, \mathbf{x}_2, \mathbf{x}_3) = 0, \quad i \neq j \neq k, \end{aligned} \quad (\text{D1})$$

where m is the mass of identical bosons. \mathbf{x}_i denotes the position of i -th particle, and $\mathbf{r}_{ij} = \mathbf{x}_i - \mathbf{x}_j$ is relative coordinate between i -th and j -th particles. The pair-wise interaction between i -th and j -th particles is described by $U(r_{ij})$, and $U_{(4)}(\mathbf{r}_{13}, \mathbf{r}_{23})$ represents the three-body interaction among all particles. Both pair-wise and three-body interactions in finite volume are assumed to be short-range and periodic, that is to say

$$\begin{aligned} U(r) &= U(|\mathbf{r} + \mathbf{n}L|), \quad \mathbf{n} \in \mathbb{Z}^3, \\ U_{(4)}(\mathbf{r}_{13}, \mathbf{r}_{23}) &= U_{(4)}(\mathbf{r}_{13} + \mathbf{n}_1L, \mathbf{r}_{23} + \mathbf{n}_2L), \quad \mathbf{n}_{1,2} \in \mathbb{Z}^3, \end{aligned} \quad (\text{D2})$$

where L is the size of the cubic lattice. Therefore finite volume three-particle wave function must also satisfy periodic boundary condition,

$$\Phi(\mathbf{x}_1, \mathbf{x}_2, \mathbf{x}_3) = \Phi(\mathbf{x}_1 + \mathbf{n}_{\mathbf{x}_1}, \mathbf{x}_2 + \mathbf{n}_{\mathbf{x}_2}, \mathbf{x}_3 + \mathbf{n}_{\mathbf{x}_3}), \quad (\text{D3})$$

where $\mathbf{n}_{\mathbf{x}_i} \in \mathbb{Z}^3$. As suggested in [65, 66], it may be more convenient to consider the integral representation of Eq.(D1),

$$\begin{aligned} \Phi(\mathbf{x}_1, \mathbf{x}_2, \mathbf{x}_3) &= \int_{L^3} \prod_{i=1}^3 d\mathbf{x}'_i \frac{1}{L^9} \sum_{\mathbf{p}_1, \mathbf{p}_2, \mathbf{p}_3} \frac{e^{i \sum_{i=1}^3 \mathbf{p}_i \cdot (\mathbf{x}_i - \mathbf{x}'_i)}}{2mE - \sum_{i=1}^3 \mathbf{p}_i^2} \\ &\times \left[\sum_{k=1}^3 U(r'_{ij}) + U_{(4)}(\mathbf{r}'_{13}, \mathbf{r}'_{23}) \right] \Phi(\mathbf{x}'_1, \mathbf{x}'_2, \mathbf{x}'_3), \end{aligned} \quad (\text{D4})$$

where $\mathbf{p}_{1,2,3} \in \frac{2\pi\mathbf{n}}{L}$, $\mathbf{n} \in \mathbb{Z}^3$. The center of mass motion of three-particle system can be factorized by

$$\Phi(\mathbf{x}_1, \mathbf{x}_2, \mathbf{x}_3) = e^{i\mathbf{P} \cdot \mathbf{R}} \phi(\mathbf{r}_{13}, \mathbf{r}_{23}), \quad (\text{D5})$$

where $\mathbf{R} = \frac{\mathbf{x}_1 + \mathbf{x}_2 + \mathbf{x}_3}{3} = \frac{\mathbf{r}_{13} + \mathbf{r}_{23}}{3} + \mathbf{x}_3$ is center of mass position of three-particle system, and $\mathbf{P} = \frac{2\pi}{L} \mathbf{d}$ with $\mathbf{d} \in \mathbb{Z}^3$ stands for the total momentum of three-particle in a periodic cubic box. $\phi(\mathbf{r}_{13}, \mathbf{r}_{23})$ is the wave function that is associated with the internal motion of three particles, and it satisfies periodic boundary condition,

$$\phi(\mathbf{r}_{13} + \mathbf{n}_1L, \mathbf{r}_{23} + \mathbf{n}_2L) = e^{-i\frac{\mathbf{P}}{3} \cdot (\mathbf{n}_1L + \mathbf{n}_2L)} \phi(\mathbf{r}_{13}, \mathbf{r}_{23}), \quad (\text{D6})$$

where $\mathbf{n}_{1,2} \in \mathbb{Z}^3$. We remark that in this work we use $(\mathbf{r}_{13}, \mathbf{r}_{23})$ to describe the internal motion of three particles, and \mathbf{x}_3 is thus associated to CM motion. So that $\int_{L^3} \prod_{i=1}^3 d\mathbf{x}'_i = \int_{L^3} d\mathbf{r}'_{13} d\mathbf{r}'_{23} d\mathbf{x}'_3$, and it resembles a two-light and one heavy three-body atomic system. Integrating out CM motion,

$$\int_{L^3} d\mathbf{x}'_3 e^{i(\mathbf{P} - \mathbf{p}_1 - \mathbf{p}_2 - \mathbf{p}_3) \cdot \mathbf{x}'_3} = L^3 \delta_{\mathbf{p}_3, \mathbf{P} - \mathbf{p}_1 - \mathbf{p}_2}, \quad (\text{D7})$$

the three-particle Lippmann-Schwinger equation, Eq.(D4), now is reduced to

$$\begin{aligned} \phi(\mathbf{r}_{13}, \mathbf{r}_{23}) &= \int_{L^3} d\mathbf{r}'_{13} d\mathbf{r}'_{23} G^{(\mathbf{P})}(\mathbf{r}_{13} - \mathbf{r}'_{13}, \mathbf{r}_{23} - \mathbf{r}'_{23}; E) \\ &\times \left[\sum_{k=1}^3 U(r'_{ij}) + U_{(4)}(\mathbf{r}'_{13}, \mathbf{r}'_{23}) \right] \phi(\mathbf{r}'_{13}, \mathbf{r}'_{23}). \end{aligned} \quad (\text{D8})$$

The three-particle Green's function is defined by

$$\begin{aligned} G^{(\mathbf{P})}(\mathbf{r}_{13}, \mathbf{r}_{23}; E) &= \sum_{\mathbf{p}_1, \mathbf{p}_2} e^{i(\mathbf{p}_1 - \frac{\mathbf{P}}{3}) \cdot \mathbf{r}_{13}} e^{i(\mathbf{p}_2 - \frac{\mathbf{P}}{3}) \cdot \mathbf{r}_{23}} \tilde{G}^{(\mathbf{P})}(\mathbf{p}_1, \mathbf{p}_2; E), \\ \tilde{G}^{(\mathbf{P})}(\mathbf{p}_1, \mathbf{p}_2; E) &= \frac{1}{L^6} \frac{1}{2mE - \sum_{i=1}^3 \mathbf{p}_i^2}, \end{aligned} \quad (\text{D9})$$

where $\mathbf{p}_{1,2} \in \frac{2\pi\mathbf{n}}{L}$, $\mathbf{n} \in \mathbb{Z}^3$, and $\mathbf{p}_3 = \mathbf{P} - \mathbf{p}_1 - \mathbf{p}_2$.

Following the same procedures as described in Section II, only two independent scattering amplitudes are required due to exchange symmetry of three-particle wave

function,

$$\begin{aligned}
T_{(2)}^{(\mathbf{P})}(\mathbf{k}_1, \mathbf{k}_2) &= - \int_{L^3} d\mathbf{r}_{13} d\mathbf{r}_{23} e^{-i(\mathbf{k}_1 - \frac{\mathbf{P}}{3}) \cdot \mathbf{r}_{13}} e^{-i(\mathbf{k}_2 - \frac{\mathbf{P}}{3}) \cdot \mathbf{r}_{23}} \\
&\quad \times U(r_{13}) \phi(\mathbf{r}_{13}, \mathbf{r}_{23}), \\
T_{(4)}^{(\mathbf{P})}(\mathbf{k}_1, \mathbf{k}_2) &= - \int_{L^3} d\mathbf{r}_{13} d\mathbf{r}_{23} e^{-i(\mathbf{k}_1 - \frac{\mathbf{P}}{3}) \cdot \mathbf{r}_{13}} e^{-i(\mathbf{k}_2 - \frac{\mathbf{P}}{3}) \cdot \mathbf{r}_{23}} \\
&\quad \times U_{(4)}(\mathbf{r}_{13}, \mathbf{r}_{23}) \phi(\mathbf{r}_{13}, \mathbf{r}_{23}). \quad (\text{D10})
\end{aligned}$$

Two amplitudes, $T_{(2)}^{(\mathbf{P})}$ and $T_{(4)}^{(\mathbf{P})}$, satisfy equations,

$$\begin{aligned}
T_{(2)}^{(\mathbf{P})}(\mathbf{k}_1, \mathbf{k}_2) &= \sum_{\mathbf{p}_1} \tilde{U}(|\mathbf{k}_1 - \mathbf{p}_1|) L^3 \tilde{G}^{(\mathbf{P})}(\mathbf{p}_1, \mathbf{k}_2; E) \\
&\times \left[T_{(2)}^{(\mathbf{P})}(\mathbf{p}_1, \mathbf{k}_2) + T_{(2)}^{(\mathbf{P})}(\mathbf{k}_2, \mathbf{p}_1) \right. \\
&\quad \left. + T_{(2)}^{(\mathbf{P})}(\mathbf{p}_1, \mathbf{P} - \mathbf{p}_1 - \mathbf{k}_2) + T_{(4)}^{(\mathbf{P})}(\mathbf{p}_1, \mathbf{k}_2) \right], \quad (\text{D11})
\end{aligned}$$

and

$$\begin{aligned}
T_{(4)}^{(\mathbf{P})}(\mathbf{k}_1, \mathbf{k}_2) &= \sum_{\mathbf{p}_1, \mathbf{p}_2} \tilde{U}_{(4)}(\mathbf{k}_1 - \mathbf{p}_1, \mathbf{k}_2 - \mathbf{p}_2) \\
&\times \tilde{G}^{(\mathbf{P})}(\mathbf{p}_1, \mathbf{p}_2; E) \left[T_{(2)}^{(\mathbf{P})}(\mathbf{p}_1, \mathbf{p}_2) + T_{(2)}^{(\mathbf{P})}(\mathbf{p}_2, \mathbf{p}_1) \right. \\
&\quad \left. + T_{(2)}^{(\mathbf{P})}(\mathbf{p}_1, \mathbf{p}_3) + T_{(4)}^{(\mathbf{P})}(\mathbf{p}_1, \mathbf{p}_2) \right], \quad (\text{D12})
\end{aligned}$$

where $\mathbf{p}_3 = \mathbf{P} - \mathbf{p}_1 - \mathbf{p}_2$, and \tilde{U} and $\tilde{U}_{(4)}$ are the Fourier transform of interaction potentials U and $U_{(4)}$ respectively. Non-relativistic three-particle dynamical equations, Eq.(D11) and Eq.(D12), resemble their relativistic counterparts, Eq.(25) and Eq.(26), excepts some relativistic kinematic factors.

-
- [1] J. Kambor, C. Wiesendanger, and D. Wyler, *Nucl. Phys.* **B465**, 215 (1996), arXiv:hep-ph/9509374 [hep-ph].
- [2] A. V. Anisovich and H. Leutwyler, *Phys. Lett.* **B375**, 335 (1996), arXiv:hep-ph/9601237 [hep-ph].
- [3] S. P. Schneider, B. Kubis, and C. Ditsche, *JHEP* **02**, 028 (2011), arXiv:1010.3946 [hep-ph].
- [4] K. Kampf, M. Knecht, J. Novotny, and M. Zdrahal, *Phys. Rev.* **D84**, 114015 (2011), arXiv:1103.0982 [hep-ph].
- [5] P. Guo, I. V. Danilkin, D. Schott, C. Fernández-Ramírez, V. Mathieu, and A. P. Szczepaniak, *Phys. Rev.* **D92**, 054016 (2015), arXiv:1505.01715 [hep-ph].
- [6] P. Guo, I. V. Danilkin, C. Fernández-Ramírez, V. Mathieu, and A. P. Szczepaniak, *Phys. Lett.* **B771**, 497 (2017), arXiv:1608.01447 [hep-ph].
- [7] G. Colangelo, S. Lanz, H. Leutwyler, and E. Passemar, *Phys. Rev. Lett.* **118**, 022001 (2017), arXiv:1610.03494 [hep-ph].
- [8] V. Efimov, *Phys. Lett.* **33B**, 563 (1970).
- [9] E. Braaten and H. W. Hammer, *Phys. Rept.* **428**, 259 (2006), arXiv:cond-mat/0410417 [cond-mat].
- [10] M. V. Zhukov, B. V. Danilin, D. V. Fedorov, J. M. Bang, I. J. Thompson, and J. S. Vaagen, *Phys. Rept.* **231**, 151 (1993).
- [11] H. W. Hammer, C. Ji, and D. R. Phillips, *J. Phys.* **G44**, 103002 (2017), arXiv:1702.08605 [nucl-th].
- [12] H.-W. Hammer, A. Nogga, and A. Schwenk, *Rev. Mod. Phys.* **85**, 197 (2013), arXiv:1210.4273 [nucl-th].
- [13] E. Epelbaum, H.-W. Hammer, and U.-G. Meissner, *Rev. Mod. Phys.* **81**, 1773 (2009), arXiv:0811.1338 [nucl-th].
- [14] H. W. Hammer, S. König, and U. van Kolck, (2019), arXiv:1906.12122 [nucl-th].
- [15] E. H. Fradkin, C. Nayak, A. Tsvelik, and F. Wilczek, *Nucl. Phys.* **B516**, 704 (1998), arXiv:cond-mat/9711087 [cond-mat].
- [16] S. Aoki *et al.* (CP-PACS), *Phys. Rev.* **D76**, 094506 (2007), arXiv:0708.3705 [hep-lat].
- [17] X. Feng, K. Jansen, and D. B. Renner, *Phys. Rev.* **D83**, 094505 (2011), arXiv:1011.5288 [hep-lat].
- [18] C. B. Lang, D. Mohler, S. Prelovsek, and M. Vidmar, *Phys. Rev.* **D84**, 054503 (2011), [Erratum: *Phys. Rev.* **D89**, no.5, 059903 (2014)], arXiv:1105.5636 [hep-lat].
- [19] S. Aoki *et al.* (CS), *Phys. Rev.* **D84**, 094505 (2011), arXiv:1106.5365 [hep-lat].
- [20] J. J. Dudek, R. G. Edwards, and C. E. Thomas, *Phys. Rev.* **D86**, 034031 (2012), arXiv:1203.6041 [hep-ph].
- [21] J. J. Dudek, R. G. Edwards, and C. E. Thomas (Hadron Spectrum), *Phys. Rev.* **D87**, 034505 (2013), [Erratum: *Phys. Rev.* **D90**, no.9, 099902 (2014)], arXiv:1212.0830 [hep-ph].
- [22] D. J. Wilson, J. J. Dudek, R. G. Edwards, and C. E. Thomas, *Phys. Rev.* **D91**, 054008 (2015), arXiv:1411.2004 [hep-ph].
- [23] D. J. Wilson, R. A. Briceño, J. J. Dudek, R. G. Edwards, and C. E. Thomas, *Phys. Rev.* **D92**, 094502 (2015), arXiv:1507.02599 [hep-ph].
- [24] J. J. Dudek, R. G. Edwards, and D. J. Wilson (Hadron Spectrum), *Phys. Rev.* **D93**, 094506 (2016), arXiv:1602.05122 [hep-ph].
- [25] S. R. Beane, W. Detmold, T. C. Luu, K. Orginos, M. J. Savage, and A. Torok, *Phys. Rev. Lett.* **100**, 082004 (2008), arXiv:0710.1827 [hep-lat].
- [26] W. Detmold, M. J. Savage, A. Torok, S. R. Beane, T. C. Luu, K. Orginos, and A. Parreno, *Phys. Rev.* **D78**, 014507 (2008), arXiv:0803.2728 [hep-lat].
- [27] B. Hörz and A. Hanlon, *Phys. Rev. Lett.* **123**, 142002 (2019), arXiv:1905.04277 [hep-lat].
- [28] M. Lüscher, *Nucl. Phys.* **B354**, 531 (1991).
- [29] K. Rummukainen and S. A. Gottlieb, *Nucl. Phys.* **B450**, 397 (1995), arXiv:hep-lat/9503028 [hep-lat].
- [30] N. H. Christ, C. Kim, and T. Yamazaki, *Phys. Rev.* **D72**, 114506 (2005), arXiv:hep-lat/0507009 [hep-lat].
- [31] V. Bernard, M. Lage, U.-G. Meißner, and A. Rusetsky, *JHEP* **08**, 024 (2008), arXiv:0806.4495 [hep-lat].
- [32] S. He, X. Feng, and C. Liu, *JHEP* **07**, 011 (2005), arXiv:hep-lat/0504019 [hep-lat].

- [33] M. Lage, U.-G. Meißner, and A. Rusetsky, *Phys. Lett.* **B681**, 439 (2009), arXiv:0905.0069 [hep-lat].
- [34] M. Döring, U.-G. Meißner, E. Oset, and A. Rusetsky, *Eur. Phys. J.* **A47**, 139 (2011), arXiv:1107.3988 [hep-lat].
- [35] R. A. Briceño and Z. Davoudi, *Phys. Rev.* **D88**, 094507 (2013), arXiv:1204.1110 [hep-lat].
- [36] M. T. Hansen and S. R. Sharpe, *Phys. Rev.* **D86**, 016007 (2012), arXiv:1204.0826 [hep-lat].
- [37] P. Guo, J. Dudek, R. Edwards, and A. P. Szczepaniak, *Phys. Rev.* **D88**, 014501 (2013), arXiv:1211.0929 [hep-lat].
- [38] P. Guo, *Phys. Rev.* **D88**, 014507 (2013), arXiv:1304.7812 [hep-lat].
- [39] S. Kreuzer and H. W. Hammer, *Phys. Lett.* **B673**, 260 (2009), arXiv:0811.0159 [nucl-th].
- [40] S. Kreuzer and H. W. Hammer, *Eur. Phys. J.* **A43**, 229 (2010), arXiv:0910.2191 [nucl-th].
- [41] S. Kreuzer and H. W. Grieblhammer, *Eur. Phys. J.* **A48**, 93 (2012), arXiv:1205.0277 [nucl-th].
- [42] K. Polejaeva and A. Rusetsky, *Eur. Phys. J.* **A48**, 67 (2012), arXiv:1203.1241 [hep-lat].
- [43] R. A. Briceño and Z. Davoudi, *Phys. Rev.* **D87**, 094507 (2013), arXiv:1212.3398 [hep-lat].
- [44] M. T. Hansen and S. R. Sharpe, *Phys. Rev.* **D90**, 116003 (2014), arXiv:1408.5933 [hep-lat].
- [45] M. T. Hansen and S. R. Sharpe, *Phys. Rev.* **D92**, 114509 (2015), arXiv:1504.04248 [hep-lat].
- [46] M. T. Hansen and S. R. Sharpe, *Phys. Rev.* **D93**, 096006 (2016), [Erratum: *Phys. Rev.* D96,no.3,039901(2017)], arXiv:1602.00324 [hep-lat].
- [47] H.-W. Hammer, J.-Y. Pang, and A. Rusetsky, *JHEP* **09**, 109 (2017), arXiv:1706.07700 [hep-lat].
- [48] H. W. Hammer, J. Y. Pang, and A. Rusetsky, *JHEP* **10**, 115 (2017), arXiv:1707.02176 [hep-lat].
- [49] U.-G. Meißner, G. Ríos, and A. Rusetsky, *Phys. Rev. Lett.* **114**, 091602 (2015), [Erratum: *Phys. Rev. Lett.* 117,no.6,069902(2016)], arXiv:1412.4969 [hep-lat].
- [50] R. A. Briceño, M. T. Hansen, and S. R. Sharpe, *Phys. Rev.* **D95**, 074510 (2017), arXiv:1701.07465 [hep-lat].
- [51] S. R. Sharpe, *Phys. Rev.* **D96**, 054515 (2017), [Erratum: *Phys. Rev.* D98,no.9,099901(2018)], arXiv:1707.04279 [hep-lat].
- [52] M. Mai and M. Döring, *Eur. Phys. J.* **A53**, 240 (2017), arXiv:1709.08222 [hep-lat].
- [53] M. Mai and M. Döring, *Phys. Rev. Lett.* **122**, 062503 (2019), arXiv:1807.04746 [hep-lat].
- [54] M. Döring, H. W. Hammer, M. Mai, J. Y. Pang, §. A. Rusetsky, and J. Wu, *Phys. Rev.* **D97**, 114508 (2018), arXiv:1802.03362 [hep-lat].
- [55] F. Romero-López, A. Rusetsky, and C. Urbach, *Eur. Phys. J.* **C78**, 846 (2018), arXiv:1806.02367 [hep-lat].
- [56] P. Guo, *Phys. Rev.* **D95**, 054508 (2017), arXiv:1607.03184 [hep-lat].
- [57] P. Guo and V. Gasparian, *Phys. Lett.* **B774**, 441 (2017), arXiv:1701.00438 [hep-lat].
- [58] P. Guo and V. Gasparian, *Phys. Rev.* **D97**, 014504 (2018), arXiv:1709.08255 [hep-lat].
- [59] P. Guo and T. Morris, *Phys. Rev.* **D99**, 014501 (2019), arXiv:1808.07397 [hep-lat].
- [60] T. D. Blanton, F. Romero-López, and S. R. Sharpe, *JHEP* **03**, 106 (2019), arXiv:1901.07095 [hep-lat].
- [61] F. Romero-López, S. R. Sharpe, T. D. Blanton, R. A. Briceño, and M. T. Hansen, (2019), arXiv:1908.02411 [hep-lat].
- [62] T. D. Blanton, F. Romero-López, and S. R. Sharpe, (2019), arXiv:1909.02973 [hep-lat].
- [63] M. Mai, M. Döring, C. Culver, and A. Alexandru, (2019), arXiv:1909.05749 [hep-lat].
- [64] P. Guo, M. Döring, and A. P. Szczepaniak, *Phys. Rev.* **D98**, 094502 (2018), arXiv:1810.01261 [hep-lat].
- [65] P. Guo, (2019), arXiv:1908.08081 [hep-lat].
- [66] P. Guo and M. Döring, *Phys. Rev.* **D101**, 034501 (2020), arXiv:1910.08624 [hep-lat].
- [67] P. Guo, (2020), arXiv:2002.04111 [hep-lat].
- [68] L. D. Faddeev, *Sov. Phys. JETP* **12**, 1014 (1961), [*Zh. Eksp. Teor. Fiz.* 39,1459(1960)].
- [69] L. D. Faddeev, *Mathematical Aspects of the Three-body Problem in the Quantum Scattering Theory* (IPST, 1963).
- [70] A. Rusetsky, in *37th International Symposium on Lattice Field Theory (Lattice 2019) Wuhan, Hubei, China, June 16-22, 2019* (2019) arXiv:1911.01253 [hep-lat].
- [71] N. N. Khuri and S. B. Treiman, *Phys. Rev.* **119**, 1115 (1960).
- [72] J. B. Bronzan and C. Kacser, *Phys. Rev.* **132**, 2703 (1963).
- [73] I. J. R. Aitchison, *Phys. Rev.* **137**, B1070 (1965).
- [74] P. Guo, I. V. Danilkin, and A. P. Szczepaniak, *Eur. Phys. J.* **A51**, 135 (2015), arXiv:1409.8652 [hep-ph].
- [75] P. Guo, *Phys. Rev.* **D91**, 076012 (2015), arXiv:1412.3970 [hep-ph].
- [76] I. V. Danilkin, C. Fernández-Ramírez, P. Guo, V. Mathieu, D. Schott, M. Shi, and A. P. Szczepaniak, *Phys. Rev.* **D91**, 094029 (2015), arXiv:1409.7708 [hep-ph].
- [77] P. Guo, *Mod. Phys. Lett.* **A31**, 1650058 (2016), arXiv:1506.00042 [hep-ph].
- [78] J. F. Cornwell, *Group theory in physics: An introduction* (San Diego, California, USA: Academic Press, 1997).
- [79] R. Kaminski, J. R. Pelaez, and F. J. Yndurain, *Phys. Rev.* **D77**, 054015 (2008), arXiv:0710.1150 [hep-ph].
- [80] E. E. Salpeter and H. A. Bethe, *Phys. Rev.* **84**, 1232 (1951).